Laine, R. M. Nanobuilding blocks based on the [OSiO1.5]x (x=6, 8, 10) octasilsesquioxanes. J. Mater. Chem. 15, 3725–3744

ARTICLE *in* JOURNAL OF MATERIALS CHEMISTRY · AUGUST 2005

Impact Factor: 7.44 · DOI: 10.1039/b506815k

1 AUTHOR:

Richard M. Laine
University of Michigan
312 PUBLICATIONS **7,525** CITATIONS

Nanobuilding blocks based on the $[OSiO_{1.5}]_x$ (x = 6, 8, 10) octasilsesquioxanes

Richard M. Laine

Received 13th May 2005, Accepted 21st June 2005
First published as an Advance Article on the web 21st July 2005
DOI: 10.1039/b506815k

The dissolution of high surface area silica with tetralkylammonium hydroxides at concentrations greater than 0.2 M, produces polyanionic cage structures, $[R_4N^+][^-OSiO_{1.5}]_x$ or Q_x, where x = 6, 8 or 10. The value x depends on the type of alkyl or alkanol group. If R = Me or $Me_3NCH_2CH_2OH^+$ group (choline) x = 8 is favored. These silicate anions can be functionalized by reaction with chlorosilanes or siloxanes to produce $[RSiMe_2OSiO_{1.5}]_x$. The octafunctional molecules are 1.2–1.4 nm in diameter, each functional group occupies a different octant in Cartesian space and as such all functional groups are either orthogonal to or opposite each other. This highly symmetrical structure offers the opportunity to construct multiple kinds of materials one nanometer at a time in one, two or three dimensions. In this review, we discuss methods of synthesizing the polyanionic silicates, their transformation into octafunctional building blocks, "cubes," and their use in formulating polyfunctional compounds and nanocomposites therefrom. Examples of tailoring global properties by tailoring the chemistries used to link cubes are given.

Introduction

The world is now intensely interested in nanomaterials and nanotechnology for a wide variety of reasons ranging from intellectual curiosity, to potential financial rewards to fear of the unknown. From the point of view of intellectual curiosity, nanomaterials offer exciting new challenges and opportunities that extend directly from fundamental principles found in materials science. These fundamental principles suggest that there can be tremendous changes in properties if it is possible to create materials from the bottom up, one nanometer at a time. Very briefly, the two most fundamental principles in materials science state that:

Processing and intrinsic materials properties together dictate micro (nano) structure, and

Intrinsic materials properties and nanostructure together dictate global properties.

Intrinsic materials properties include: elemental composition, bond lengths and angles, oxidation states, *etc*. A third, less encompassing principle is that:

Control at the finest length scales gives the highest homogeneity, which in turn leads to the highest reproducibility, predictability, and in principle the best opportunity to tailor materials' properties.

The reason the latter principle is less encompassing is that some sets of properties are only achieved by creating composites. However, for composites, the same rules apply with regard to intrinsic materials properties, processing and control at the finest length scales. Thus, efforts to generate both single-phase materials and composites with higher degrees of homogeneity must eventually lead to studies on materials with nanosized components.

It is now recognized that the outcome of such studies will not only lead to optimization of properties for known materials, it can also lead to entirely new materials. This is predicated in part on creating nanosized components whose intrinsic properties differ significantly from bulk materials of the same composition. In part, the assembly of nanosized components will also result in large volume fractions of interfaces that can greatly affect global properties because these interfaces will have properties unrelated to the components themselves, and/or that are not predictable based on the bulk properties of the components that form the interface.

Clearly, the availability of diverse nanocomponents that are easily made and whose properties and assembly can be closely controlled could have a significant impact on the development of nanomaterials and nanotechnologies. This then represents the motivation for this review. It is extremely easy to make diverse nanocomponents based on the silsesquioxanes shown in Fig. 1, especially those based on octasilicate anions or OSAs, as we will discuss below.

Of particular importance from the perspective of nanoassembly is the fact that the octafunctional octasilsesquioxanes are 1.2–1.4 nanometers in diameter and can have functional groups in each octant in Cartesian space, either opposite or completely orthogonal to each other. This symmetry allows their assembly in one, two or three dimensions nm by nm, selectively with complete control of periodicity over very long length scales as will be shown below.

Recently, the creation of materials based on polyhedral oligomeric and OSA derived silsesquioxanes (cubes as they will be called here) has generated tremendous excitement for numerous reasons including those indicated above. Cubes and related polyhedral silsesquioxanes have been used to model

Department of Materials Science and Engineering, and the Macromolecular Science and Engineering Program, University of Michigan, Ann Arbor, MI 48109-2136, USA.
E-mail: talsdad@umich.edu

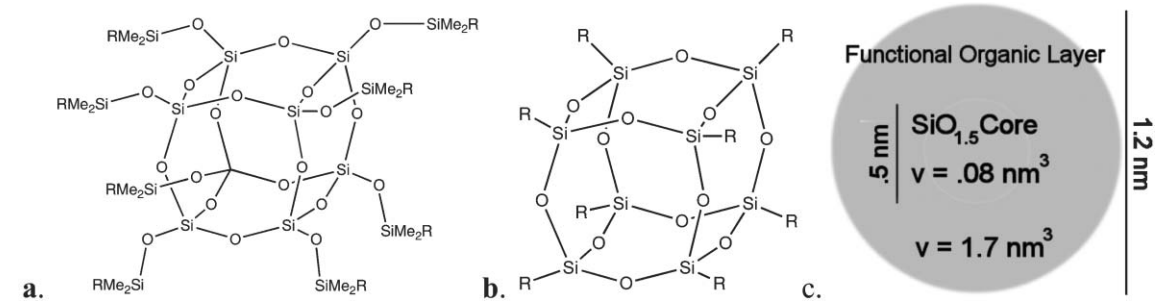

Fig. 1 Cubic silsesquioxanes. a. Q_8 (Q = SiO_4) R = H, vinyl, epoxy, 3-hydroxypropyl, aminopropyl, glycidylepoxy, ethylcyclohexylepoxy, methacrylate, *etc*. b. R_8T_8 (T = carbon-$SiO_{1.5}$) R = alkyl, alkene, acetylene, acrylate, R′X (X = halogen, –CN, amine, epoxy, ester, *etc*. R′ = R same or mixed). c. Typical sizes/volumes.[1–16]

catalytic surfaces,[1] generate new catalysts[2] and novel porous media,[3] serve as NMR standards,[4] act as novel encapsulants,[5] and as building blocks for nanocomposite materials, as will be discussed below.[6–10] As such, a number of reviews have been written on the "T" [$(RSiO_{1.5})_x$] materials.[2d,11–15]

In contrast, although the Fig. 1a, Q_8 (OSA) system was first described by Hoebbel *et al.* in 1971[16,17] and a great many studies have since been published on it and the related Q_6 and Q_{10} OSAs,[18–27] only one brief review by Hasegawa and Sakka has appeared.[18] In this current review, we focus on the use of Q_x systems as building blocks for nanostructured materials. However, their utility extends from their ease of synthesis. Consequently, we begin by discussing Q_x (x = 6, 8, 10) formation in aqueous alcoholic solutions then discuss their derivatization and finish with a discussion of their utility in formulating and processing nanocomposite materials.

Formation and stability of Q_x species

Many of the studies on the formation of Q_x species concern the relative stability of the various forms with respect to concentration, temperature and counter ions in aqueous and/or aqueous alcoholic media.[17–27] Table 1 lists some of the relevant findings and data. Of importance is the fact that Q_x structures are very minor constituents of alkali silicate solutions made under identical conditions.[24,28] Thus, alkyl ammonium counter ions are necessary to the formation of Q_x species. Furthermore, the introduction of combinations of alkali hydroxides with alkylammonium hydroxides thwarts the formation of Q_x species if the alkali concentrations are significant.[22,24]

In general, the formation of cage structures is favored by $\geqslant$1 : 1 R_4N : Si stoichiometries that form at the expense of monomers, dimers, three or four-membered rings, which can be observed at low silicate concentrations but give way to Q_x structures at concentrations >0.2 M and are generally completely Q_8 when concentrations are >0.5 M with $Me_3NCH_2CH_2OH$ and/or Me_4N counter ions. Hasegawa *et al.*[24] have demonstrated that water is essential to the formation of the cage structure as discussed in more detail below. Finally, alkylammonium surfactants used in amine template syntheses of zeolites and mesoporous materials appear to generate Q_8 anions as intermediates in the process.[29] However, it is important to note that there are contrasting opinions about whether Q_x species actually play a role in the formation of zeolite cages.[30]

Despite the extensive studies on these materials, there has been no discussion concerning possible mechanisms of formation. We have long been interested in the dissolution of silica as a method of directly forming silicon containing chemicals and polymers.[31,32] As such, we were recently motivated to study the kinetics of rice hull ash dissolution and OSA formation using Me_4NOH and $[Me_3NCH_2CH_2OH]OH$ based on this older literature. These studies provide a picture of the formation process.

Thus the many published studies on the formation of Q_x species by reaction of high surface area amorphous silica with various R_4NOH species coupled with the ready availability of rice hull ash (RHA) provided the impetus to extend OSA synthesis to RHA.[33] Yearly RHA production is estimated to be $\approx$3 million tons and is currently considered a useless waste product of rice production (80 M ton y^{-1}). Most RHA consists of 80–98 wt% amorphous silica with 20–2 wt% amorphous carbon with surface areas of 20–50 m^2 g^{-1} making it potentially a very reactive, low cost alternative to silica gel. In addition to looking at RHA for its low cost, its reactivity at

Table 1 Formation of $[^-OSiO_{1.5}]_x$ species as a function of counter ion in aqueous media

Anion	$R_{4-x}N$	Si : N	Conc.	^{29}Si ppm	Remarks	Ref.
$[^-OSiO_{1.5}]_6$	Et, x = 0	1 : 1	>0.8 M	−88.2		18
$[^-OSiO_{1.5}]_6$	nPr, x = 0	1 : 1	1 M	−88.2	At −1 °C	19
$[^-OSiO_{1.5}]_8$	Me, x = 0	1 : 1		−98.7		19
$[^-OSiO_{1.5}]_{10}$	nBu, x = 0	1 : 1			Si : N 1 : 4 favors Q_6	17,20
$[^-OSiO_{1.5}]_6/[OSiO_{1.5}]_8$	Me_3, $(CH_2)_2OH$ $(CH_2)_3OH$	1 : 1	>1 M		Mixture favors Q_8	21
$[^-OSiO_{1.5}]_6/[OSiO_{1.5}]_8$	Et_3, $(CH_2)_2OH$ or $(CH_2)_3OH$	1 : 1	>1 M		Mixture favors Q_8	26
$[^-OSiO_{1.5}]_7[^-OAlO_{1.5}]/[OSiO_{1.5}]_8$	Me_3, $(CH_2)_2OH$ + Al^{3+}	1 : 1	>1 M		Aluminosilicate cubes observed	26
$[^-OSiO_{1.5}]_2[HOSiO_{1.5}]_6$	nBu	0.28 : 1	low			20

ambient was used to assess the possible involvement of Q_x species in biosilicification processes.[34–41]

On this basis, the effects of changes in selected variables on the dissolution of 22 m^2 g^{-1} rice hull ash that was ≈95 wt% amorphous silica and 5 wt% amorphous carbon were examined.[33] The production of OSA during the dissolution process, reaction (1), was determined by conversion of the OSA to the octahydridodimethylsiloxysilsesquioxane cube, OHS, as per reaction (2).

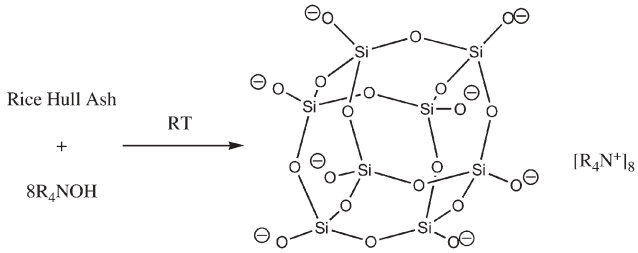

(1)

This study, which is detailed elsewhere,[33] demonstrates a direct dependence of dissolution on [Me_4NOH] as shown in Fig. 2. Dissolution asymptotes at one equivalent of base per SiO_2 available for dissolution. The water dependence, shown in Fig. 3, asymptotes at 4–5 equivalents of water per SiO_2 for Me_4N^+ and 3 equivalents per $(Me_3NCH_2CH_2OH)^+$ (not shown). Finally Fig. 4 shows the temperature dependence for the dissolution process.

The 40° and 60 °C one and two day data can be used to calculate an E_a for the dissolution process of 5 ± 1 kcal mol^{-1} of silica. This E_a is far below those found for alkali or amine base promoted silica dissolution, which are 12–15 kcal mol^{-1} in the 150–200 °C temperature range.[31,32] Furthermore, significant dissolution occurs at room temperature where previously studied forms of silica dissolution, even with amorphous silica, occur readily only at ⩾150 °C. Hence the dissolution mechanism appears to be entirely different.

The high temperatures and E_as found for normal base promoted SiO_2 dissolution were interpreted to be related to the cleavage of Si–O bonds (≈120 kcal mol^{-1}).[31,32] It appears that the ready formation of OSAs at ambient means that Si–O bond cleavage during SiO_2 depolymerization is likely not the slow step in this process. OSA cage formation appears to be the slow step.[33]

Justification for this arises from modeling studies done by Gordon and Kudo on the condensation of silanol, Si–OH, bonds in the absence and presence of water.[34–36] They calculate 7–10 kcal mol^{-1} barriers to the condensation of silanols to form dimers, trimers, cyclic trimers and

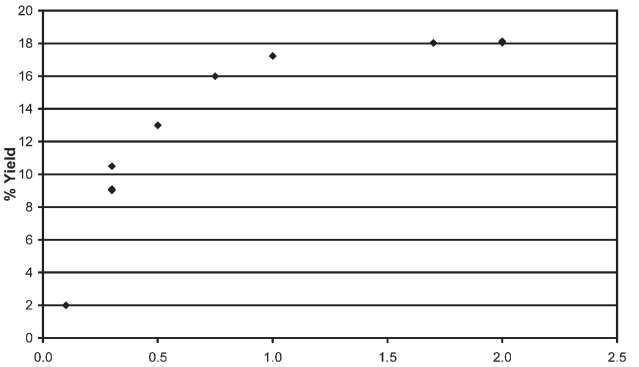

Fig. 2 RHA dissolution as a function of [Me_4NOH] at 21 °C, 3 d.

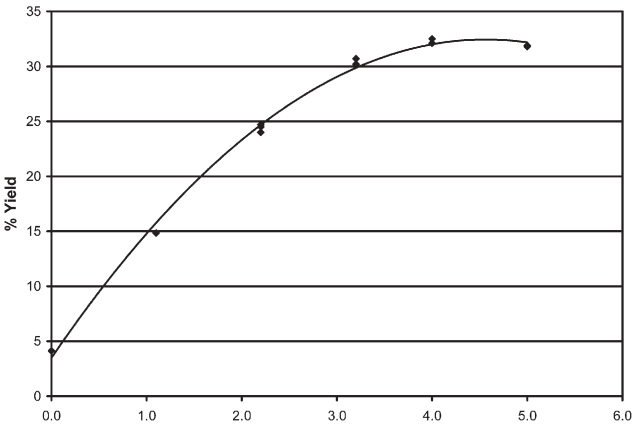

Fig. 3 [Me_4N]OH promoted RHA dissolution *vs.* moles H_2O/mole SiO_2, 18 d.

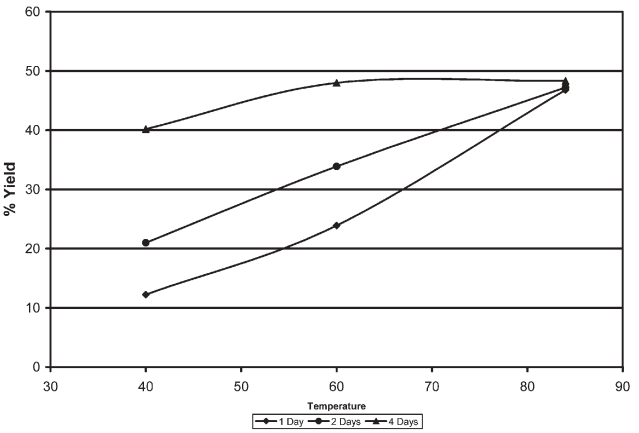

Fig. 4 Yield *vs.* temperature for RHA dissolution using standard conditions.

(2)

tetramers. However, addition of water eliminates all barriers to condensation making it highly favorable with E_as $\leqslant -10$ kcal mol^{-1}.

Given our finding of a small, 5 $\pm$ 1 kcal mol^{-1}, barrier to formation of octaanion and the strong promotional effect of water, Fig. 3; it can be argued that the small positive E_a found here differs from the very favorable processes found by Gordon and Kudo because condensation here involves anionic silanols that can be expected to exhibit some repulsive forces. Alternately, the R_4N^+ species may reorder around the anion during condensation processes and also contribute to the barrier observed. The choline OSA single crystal structure is shown in Fig. 5.[33]

The earlier work on Q_x formation[17–27] coupled with the fact that OSAs appear to form during zeolite and mesoporous materials syntheses,[29,30] and our recent studies,[33] suggest that there is considerable driving force for Q_x formation, such that it might occur even in nature. The literature on biosilicification processes, *e.g.* the processes whereby diatoms extract silicic acid [$Si(OH)_4$] at parts-per-million from water and concentrate it millions of times to create reservoirs of 0.3–0.5 M soluble silica used in creating intricately structured silica shells, lends credence to this idea.[37–44]

The likelihood of OSAs or other Q_x species forming during the biosilicification process seems to be supported by the following observations. The choline structure is very similar to hydroxyamino acids found in sponge filament proteins.[38–42] The identical structure is part of ε-*N*,*N*,*N*-trimethyl-γ-hydroxylysine found in silafins.[41] In addition, Sumper *et al.* recently demonstrated that the polypropylamine structures also found in silafins contain trimethylammonium end units reminiscent of the choline and tetramethylammonium units found here.[42] Furthermore, the biosilicification literature indicates that some as yet unknown form of silica is stored within silica transport (STV) and silica deposition vesicles (SDV) at concentrations of >0.3 M at near neutral pHs where silicic acid itself would polymerize. A further key clue also identified by Sumper *et al.* is that silafin silica deposition only seems to occur when the hydroxylysine units are phosphorylated, but not without phosphorylation.

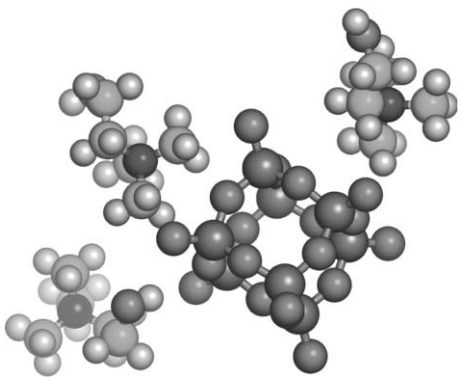

Fig. 5 Single crystal structure of $[OSiO_{1.5}]_8[Me_3NCH_2CH_2OH]_8 \cdot 24H_2O$. Waters of crystallization and additional cholines not shown to provide a better view of the octaanion.

Although studied extensively, this problem remains unresolved. One possibility is that the silica is stored as neutral species with Si–O–C bonds.[37,43,44] Other evidence suggests that silica might be stored and transported as penta- and/or hexacoordinated species (with Si–O–C bonds) formed between sugars and silica or silicic acid. However, still other studies find limited support for formation of Si–O–C species[43] and theoretical calculations suggest that hypercoordination is thermodynamically less favored in biological environments than tetracoordinate silicon.[44]

Given that Q_x species:

• form in aqueous and aqueous/alcoholic media at ambient temperatures, at slightly basic or near neutral conditions,[20,23,45,46]

• are the preferred form of anionic silicates at concentrations >0.2 M for most conditions studied, and

• form exclusively in the presence of ammonium cations similar to those found in diatoms in environments associated with the biosilicification process, suggests that

Q_x species could be "missing links" in selected forms of biosilicification, processes whereby megatons of dissolved silica are fixed each year. If correct, this information may offer considerable value. Because diatoms deposit silica in the form of nanometer size particles, at ambient in highly complex shapes, knowledge of these processes may offer potential for the low temperature construction of complex micro and nanostructures for selected nanotechnologies[47] and for energy efficient and "green" chemical processing of silica.

The ease with which Q_x species are formed, especially OSAs, their perfect size ($\approx$1 nm diameter) combined with the potential to be functionalized eight-fold where each functional group occupies a different octant in Cartesian space appears to offer exceptional opportunities to create new materials nanometer by nanometer. The key to their utility comes not from their easy synthesis, but from functionalization of the Q_x species. This turns out to be somewhat difficult because the anionic oxygen is not particularly reactive.

In principle, negatively charged oxygens should be excellent nucleophiles allowing facile functionalization. However, the combination of the protective alkylammonium counter ions coupled with the high ordering of the waters of crystallization make it quite difficult to functionalize the Q_x species. They do not react with alkyl halides, tosylates, anhydrides or related substrates normally very reactive towards nucleophilic attack. The only known method of functionalizing these materials is *via* silylation. The most common methods are those shown in reactions (2)–(4) using methods similar to those of Lentz.[48] Based on these two types of reactions, a large number of derivatives have been described in early work by a number of groups in both the open and patent literature.[49–53] A recent paper by Hoebbel *et al.* provides a comprehensive list of the types of compounds made *via* these methods.[54] There is also a report by Harrison *et al*. on the preparation of analogous Q_6 equivalent to OHS and the transformation of that product into the bromo analog.[55] A recent paper by Auner *et al.* provides single crystal structures, coupled with MALDI-TOF analyses of a number of the $(RMe_2SiO)_xQ_x$ structures where R = H, Me, vinyl.[56]

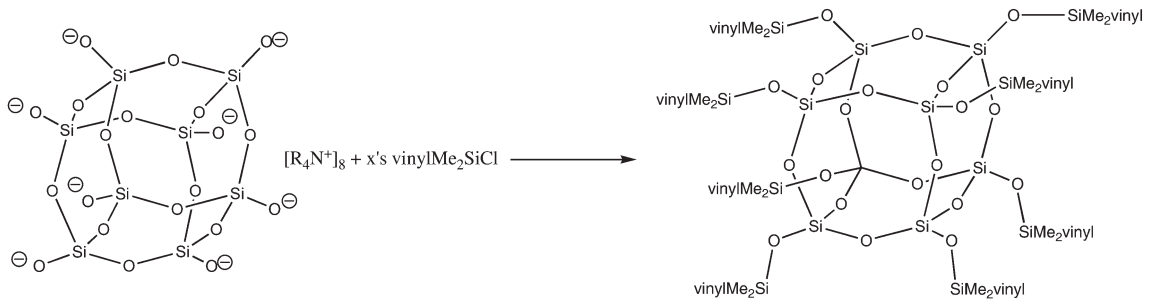

(3)

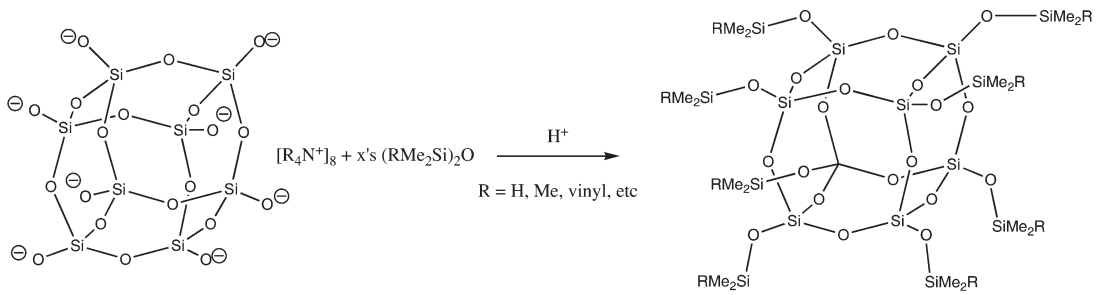

(4)

It is also important to note that by using mixtures of RMe_2SiCl, mixed R groups *e.g.* cages containing both Si–vinyl and Si–H groups can be made.[57] Like all efforts to produce Q_x species with functionalities less than "x", the resulting products will be $(RMe_2SiOSiO_{1.5})_y(ZOSiO_{1.5})_{x-y}$ where Z is either –H from the initial Q_x species or Z = $R'Me_2SiO$ from another starting chlorosilane reactant. Here "y" is often equal to the number of equivalents added to produce mixed functionality. However, the material produced typically consists of a statistical average centered on the value "y". But, if the reactivity of one added component is much less than another added at the same time, then the ratio of "y" to "$x - y$" species will reflect this difference in reactivity.

Of all of the possible products readily available from reactions (2)–(4),[49–63] OHS produced in reaction (2) and the vinyl equivalent, OVS (reaction (3), R = vinyl) represent the most common starting points for further functionalization to create novel 3-D polyfunctional materials of value in their own right or for use as "nanobuilding blocks." This is simply because the intermediates RMe_2SiCl (R = H, vinyl) are relatively low cost and the reactions have been optimized to give yields in excess of 80%. Furthermore, hydrosilylation is a common and well-understood method of converting Si–H groups to multiple other functionalities. Finally, it is also possible to exchange functionality by simple exchange reactions:[64]

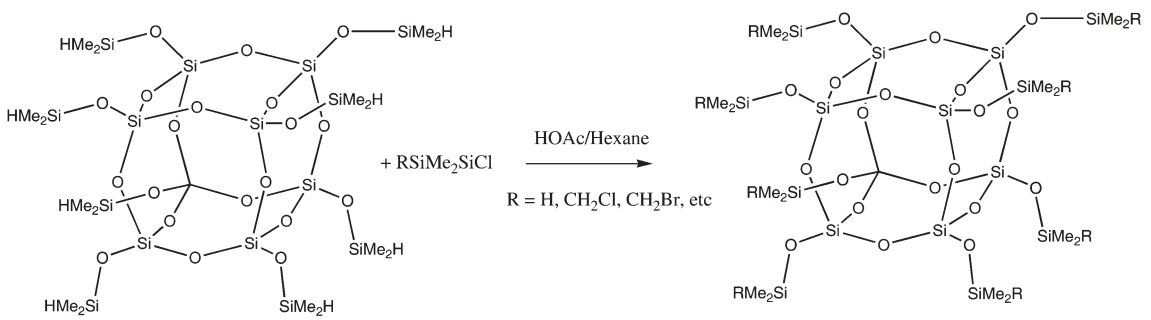

(5)

However, the majority of the literature concerning the chemistry and processing of Q_x species centers on the chemistry of OHS and/or OVS. In the following sections we discuss first some of the standard types of polyfunctional molecules that can be made from OVS and OHS and then move on to nanocomposite materials.

Polyfunctional molecules

Liquid crystalline materials

One of the first reports, by Kruezer *et al.*, on the functionalization of OHS, involved the addition of mesogens to explore the similarities and or differences between liquid crystalline materials obtained by functionalizing polysiloxanes, which provides a flexible backbone, and those using a rigid cage structure as the core.[58] This work was followed later by efforts by Mehl *et al.*, Saez and Goodby, Sellinger *et al.* and Zhang *et al.*[59–63] The properties of some selected liquid crystalline cubes are listed in Table 2.

In all instances, it is assumed that the cube mesogens can form either bundle structures where interdigitation occurs to form "super" rigid rod structures or double ring discotic structures as suggested in Fig. 6. In general, those cubes with more flexible spacers have lower melting and clearing temperatures.

Table 2 Properties of selected liquid crystalline materials made from $(HSiMe_2Q)_x$

Q_x, x =	R group	Phase[a]	Comments	Ref.
8	$(CH_2)_{10}CO_2Chol$	C 128 (G 46) S_A157 I		57
6	$(CH_2)_{10}CO_2Chol$	C 108, 160 I		57
8	$(CH_2)_3OPhCO_2$-*p*-PhCN	C 119 S_A 146 I		57
8	$CH_2)_3OPhCO_2Ph$-*p*-PhCN	G 102 S_X 127 S_A >300 I		57
10	$(CH_2)_{10}CO_2Chol$	C 122 (G 51) S_A 164 I		57
10	$(CH_2)_{10}CO_2$-*p*-$PhCO_2Chol$	C 115 (G 87) S_A 262 I		57
8	**I**-$[(CH_2)_3O]_2$-*p*-$PhCO_2$-*p*-$C_6H_4C_6H_5$	C 127, 138 I	Ave. substitution 5	61
8	**II**-$[(CH_2)_3O]_2$-*p*-$PhCO_2$-*p*-$C_6H_4C_6H_4OMe$	C 110 S_A 174, 181 N 189 I	Ave. substitution 5	61
8	**III**-$[(CH_2)_3O][(CH_2)_2O]_2$-*p*-$PhCO_2$-*p*-$C_6H_4C_6H_5$	C 72 S_A 103, 113 I	Ave. substitution 5	61
8	**IV**-$[(CH_2)_3O][(CH_2)_2O]_2$-*p*-$PhCO_2$-*p*-$C_6H_4C_6H_4OMe$	C 83 N 157 S_A 154 I	Ave. substitution 5	61

[a] C = crystalline, G = glassy, I = isotropic, S = smectic, N = nematic.

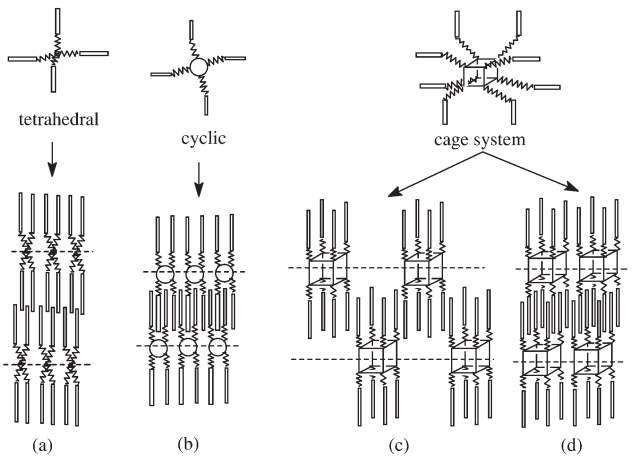

Fig. 6 LC oligomers of restricted topologies and their packing models.[62,63]

The X-ray powder diffraction patterns for the *d*-spacings of the S_A phases for reference 59 compounds combined with modeling studies indicate overlapping of the LC mesogens in the S_A layers such that the first order *d*-spacing are about equal to the mesogen length plus the cube width. This suggests interdigitation of the aromatic mesogens between neighboring layers, similar to the model proposed by Kreuzer *et al*. and Mehl *et al.* as shown in Fig. 6(c) and (d).[58–61] Furthermore, alignment in a 10 Hz electric field indicates (both for nematic and smectic phases) that the mesogens align perpendicularly to the field suggesting negative dielectric anisotropy.

Novel functional groups

Some of the more interesting functional groups that have been added to the OHS and OVS materials include some of those reported briefly by Jutzi *et al* as illustrated in Fig. 7.[65] These are in addition to other compounds mentioned in the recent Hoebbel *et al.* paper.[54]

Because these compounds can be modified to provide solubility and stability in a wide variety of environments, the ability to append mixed functionality as discussed above offers the potential for multiple synthetic strategies. For example, the high density of boron (80 per cube) in the 1,2-*cis*-dicarbadodecarborane unit in Fig. 7 suggests applications for boron neutron capture therapy.[66] The polyferrocene system could be used as a multielectron oxidant if all the ferrocenes can be converted to ferrocenium ions or for producing materials with magnetic ordering if only partial oxidation of the ferrocenes occurs.[67] A paper by Moran *et al.*[68] describes the synthesis of the related ethyl-linked ferrocene made by reaction of OHS with vinylferrocene and copolymers made using 1,1-divinylferrocene. These polymers were used to make robust polyferrocenyl electroactive coatings on electrodes, another potential application for these materials. In addition, the presence of multiple metal sites offer the opportunity to develop multisite catalysts for a wide variety of applications as discussed by Hanssen *et al.*[2d]

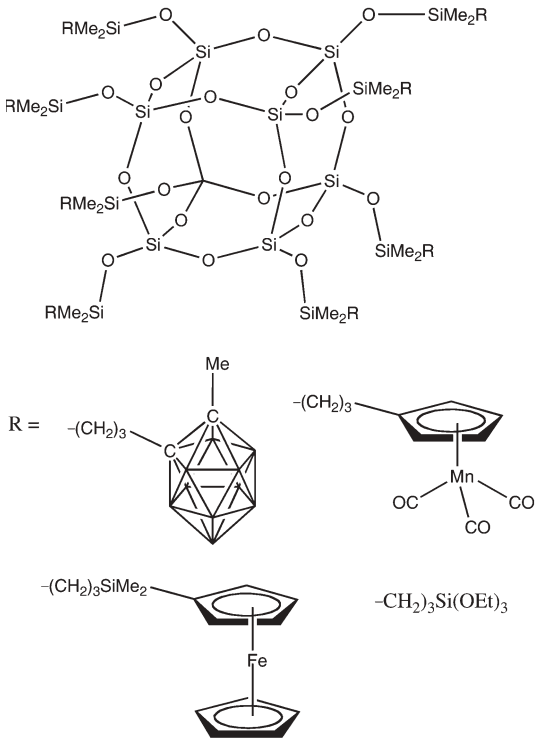

Fig. 7 Octafunctional Q_8MR materials made by hydrosilylation of the corresponding allyl derivatives using either Karstedt's or Spier's catalysts.[65]

The work by Hoebbel *et al.* on the synthesis of a perfluorinated cube as per reaction (6) leads to a transparent liquid. By using a mixture of the perfluoromethylmethacrylate and the tri-methoxysilylmethylmethyacrylate equivalent, reaction (7), coating systems were created that (following partial hydrolysis) form excellent hydrophobic coatings on glass substrates.

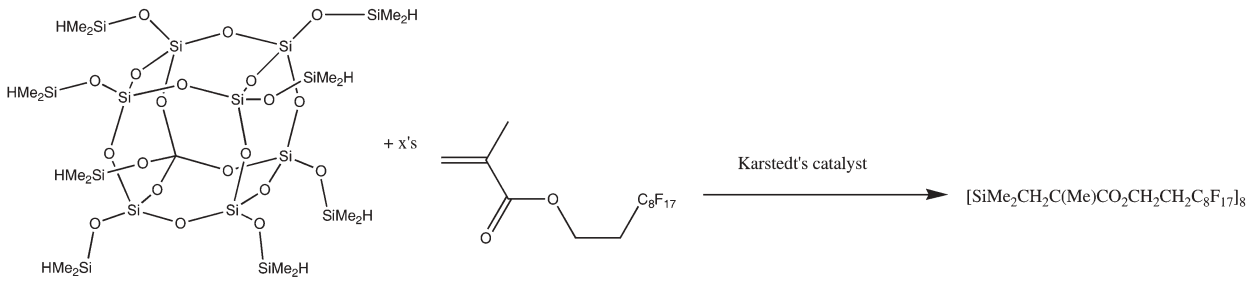

(6)

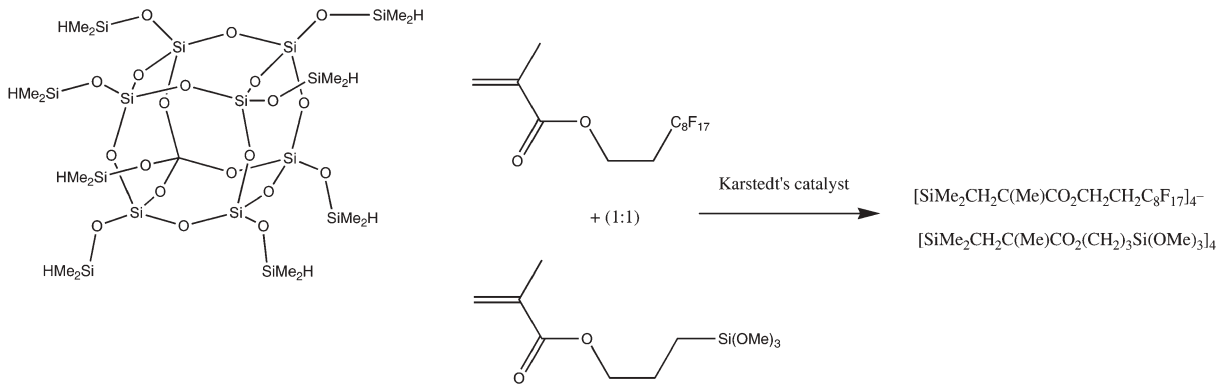

(7)

These coatings offer surface tensions lower than coatings made with the $C_8F_{17}Si(OMe)_3$ alone (22 *vs.* 24 mN m^{-1}) and contact angles of $\approx 100^\circ$ *vs.* 80° for coatings made from the pure silane. Hoebbel *et al*. argue that the structure of the cube coupled with the mixed functionality causes a distorted arrangement of the perfluoroalkyl groups leading to better hydrophobicity.

As above, the composition shown in reaction (7) is an average of the statistical substitution pattern expected and found. In these systems, the methylmethacrylate double bond is used to append different functionalities on the cube with concomitant loss of methacrylate functionality. It is also possible to place reactive methacrylate groups on the cubes that retain their functionality. Two routes have been used.

Methacrylates can be produced by hydrosilylation of the propargyl methacrylate per reaction (8) to give the tetraallylmethacrylate.[69] This straightforward reaction gives high yields with dicyclopentadiene platinum dichloride [Pt(dvs)] as catalyst as it gives the desired addition across the triple bond, whereas Karstedt's catalyst gives only gels. However, addition across the triple bond gives a mix of roughly 60% alpha (silicon adds to terminal carbon) and 40% beta.

These materials are liquids at room temperature and cure thermally or photochemically to produce 3-D methacrylate nanocomposites. They are not particularly thermally stable, decomposing at temperatures near 230 °C per Fig. 8, which shows the TGA in air. The important point to be gleaned

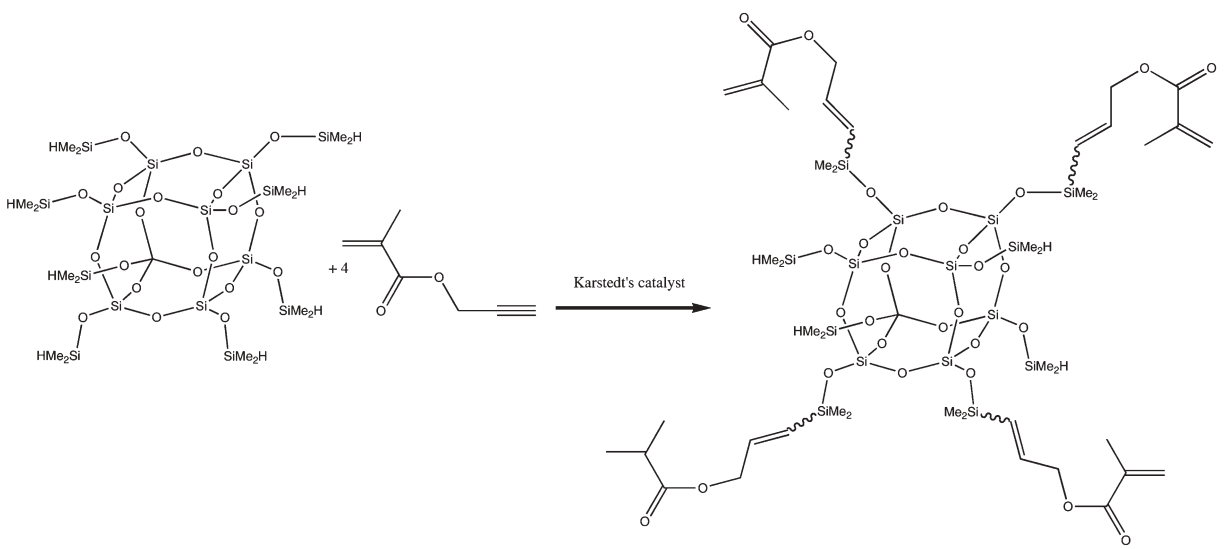

(8)

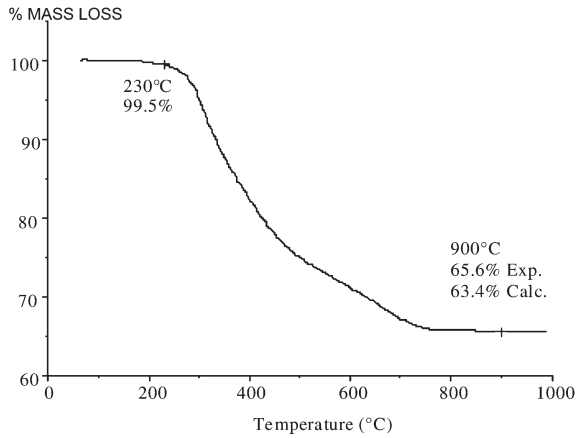

Fig. 8 TGA (air, 10 °C min^{-1}) of Q_8M_8(allylmethylmethacrylate)$_4$.

from the TGA is that although the product of reaction (7) is a statistical mixture of functional groups on the cube, the ceramic yield (SiO_2 residue at 900 °C) is very close to that calculated (65.6 *vs.* 63.4 wt%). Note that in some instances, these materials sublime in air (especially OHS) and thus ceramic yields can be low because of partial sublimation. The viscosity for the reaction (7) product is ≈300 mPa s whereas the octafunctional molecule has a viscosity of ≈900 mPa s.

The second route to methacrylates uses an atypical hydrosilylation reaction. As shown in reactions (9) and (10), the Si–H bond adds alpha across the allyl alcohol double bond without coincident reaction with the OH moiety, normally highly favored.[70] Note that the use of methacroyl anhydride gives a much cleaner product than obtained using the acid chloride.[71]

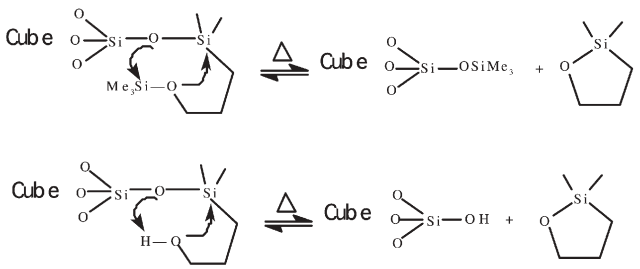

Scheme 1 Backbiting of OHPS and OSPS in polar solvents.

Allylamine can also be used to form amine functionalized cubes.[72] The intermediates OHPS and OSPS, and OMPS all undergo unique side reactions promoted by polar solvents involving backbiting elimination of cyclics, as shown in Scheme 1.[70,71]

The octamethylmethacrylate, OMPS, is also a liquid with a viscosity of <1000 mPa s at room temperature and cures with heat or light (sensitized) to give transparent and hard nanocomposites. It can be mixed with other methacrylates to formulate new types of composite systems. Its thermal stability is similar to the propargyl methacrylate derived materials.

The potential to modify these materials by changing the methyl group to, for example, butyl as done for traditional methacrylates suggests numerous opportunities for these materials based on the diverse methacrylate products currently available commercially. The one issue is the problem with backbiting that limits the stability of the intermediate octa-alcohol if polar solvents are used. Note that other unsaturated alcohols can be used successfully but only limited studies were done to explore this approach.

One remaining approach to methacrylate materials that also starts by adding novel functionality *via* hydrosilylation, is that

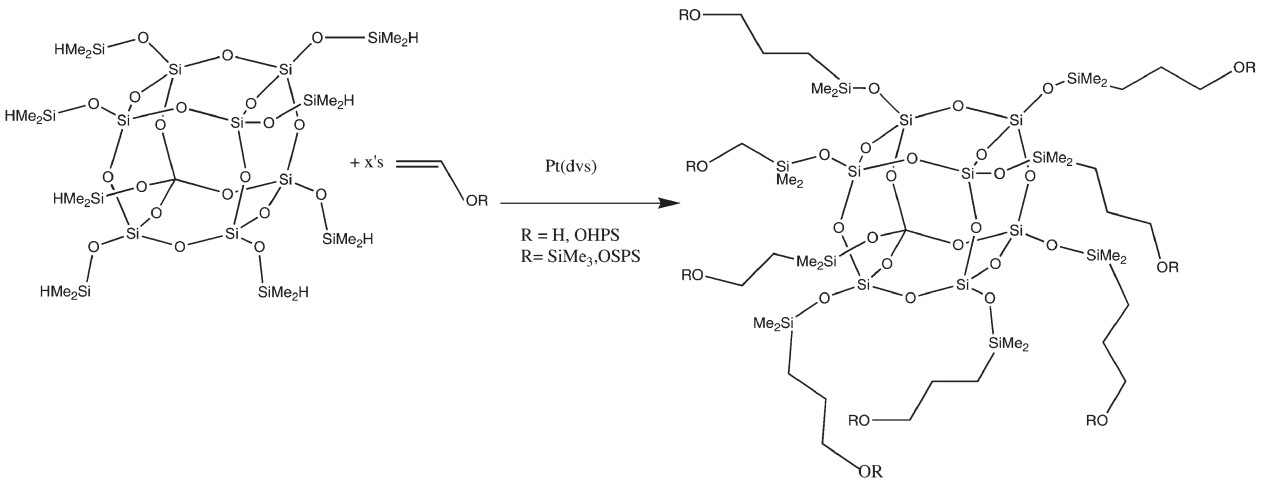

(9)

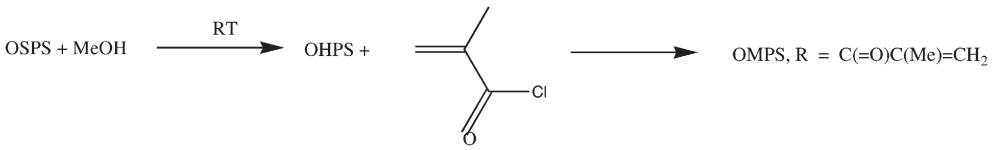

(10)

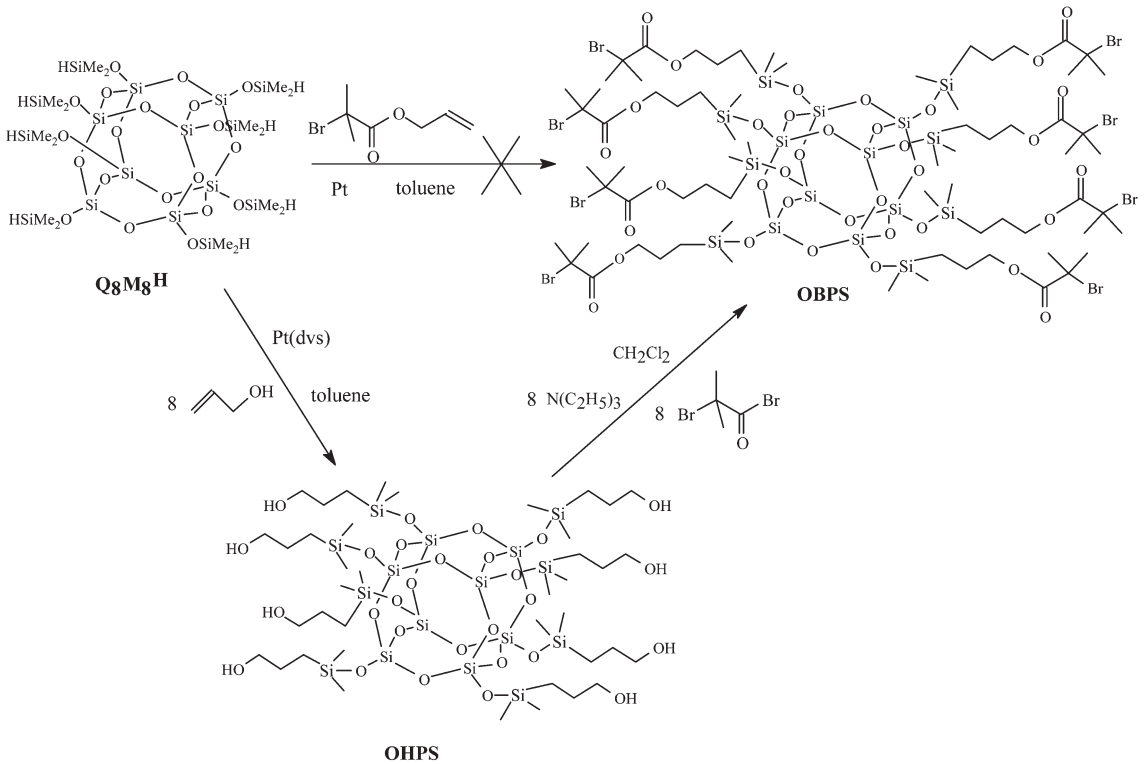

Scheme 2 Synthesis of octakis(2-bromo-2-methylpropionoxypropyldimethylsiloxy)octasilsesquioxane (OBPS) for ATRP.[74]

based on atom transfer radical polymerization (ATRP), which has recently received considerable attention because it provides access to polymers with considerable control of polydispersity.[73] We[74] and Pyun *et al.*[75] have used cubes and related polysilsesquioxanes to make star molecules using two different routes. Our approach uses OBS as the core material for ATRP, synthesized as shown in Scheme 2.

The resulting materials exhibit the expected polydispersities and properties as a function of reaction time as illustrated in Fig. 9. The glass transition temperatures (T_g) of the star polymers range from 96 to 122 °C, increasing with M_n, as expected, due to the decrease in the volume fraction of chain ends. One interesting aspect is that T_g is known to depend strongly on tacticity, *e.g.*, 105 °C for atactic PMMA, 42 °C for isotactic PMMA and 126 °C for syndiotactic PMMA.[54] The stereochemistry of PMMA produced *via* ATRP is similar to that for a free radical propagation mechanism. In addition, the T_g for linear PMMA (M_n = 22800, PDI = 1.10), prepared *via* ATRP

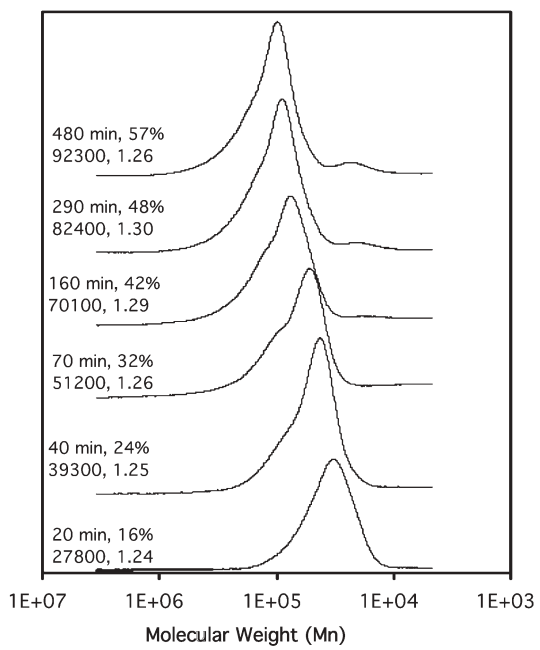

Fig. 9 GPC traces of star polymers obtained by reacting [OBPS] = 1.46 mM, [CuCl] = 11.7 mM with 290 mmol of MMa. Values represent reaction time, MMA conversion, M_n and PDI. Solvent was acetonitrile and the ligand was bipyridyl used in a 1 : 3 Cu : bipyridyl ratio at 90 °C.

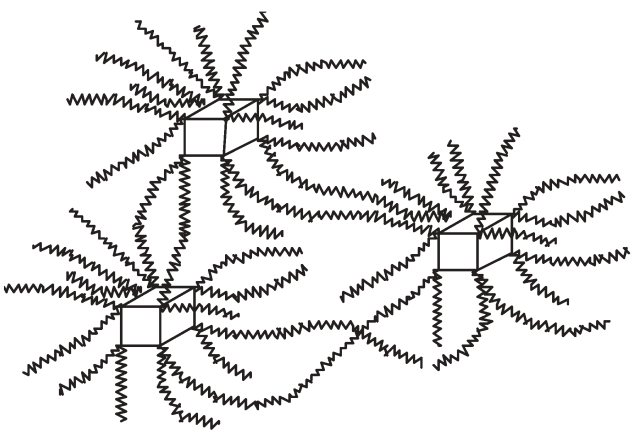

Fig. 10 Schematic of cube star clusters.

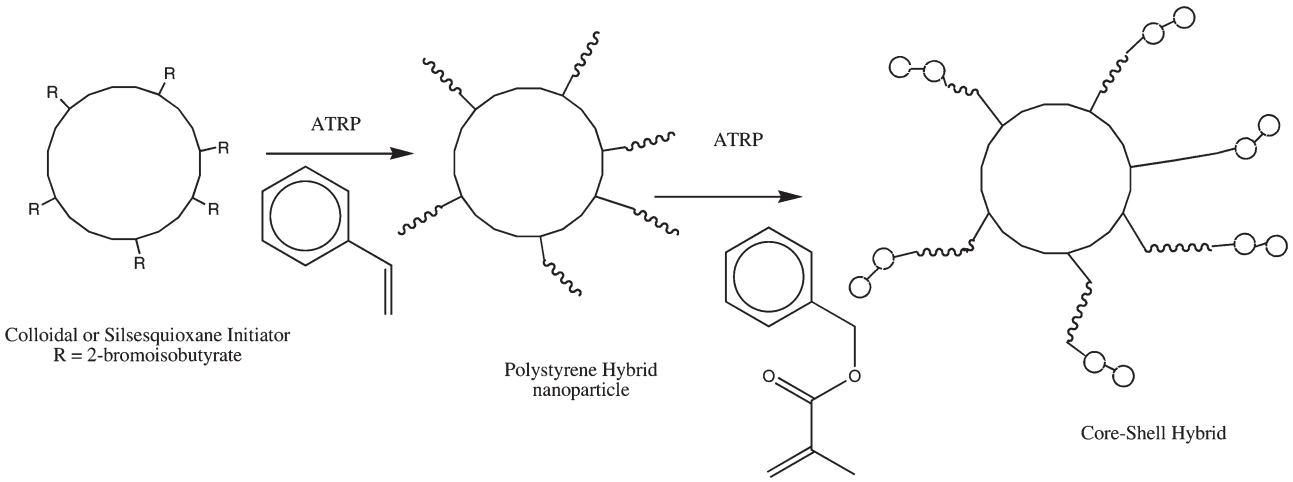

Scheme 3 ATRP used to generate block copolymers around a hard silsesquioxane core.[75]

initiated with ethyl 2-bromo-2-methylpropionate under similar reaction conditions, was determined to be 104 °C, very close to T_g for the atactic PMMA. The finding of T_gs of 120 °C at higher molecular weights suggests some unexpected control of tacticity given that syndiotactic materials offer similar T_gs; however, this possibility remains to be studied.

One other interesting aspect of these studies is that because of the relatively long-lived radicals produced in these systems, chain termination processes can be devised that produce clusters of stars as suggested by Fig. 10. The potential to create such clusters may offer opportunities to generate novel core–shell materials, new types of catalysts, filter systems, or systems equivalent to dendrimers with similar chemical properties but with hard cores. Also, note that these cores can be dissolved out with HF as discussed below.

Preliminary studies wherein hydroxymethylmethacrylate was added late in the reaction, indicated potential to make block copolymers from OBS with quite different properties than the simple PMMA stars and suggest novel avenues of study based on what is already done with linear ATRP generated polymers.[73]

One such example was reported by Pyun *et al*., Scheme 3,[75] who generate a functionalized silsesquioxane with essentially the same initiator as used above but now react styrene to form a polystyrene block first and then benzylacrylate to make a block copolymer wherein atomic force microscopy done in tapping mode demonstrates core–shell behavior with different responses to the AFM arising as a consequence of the polystyrene blocks being glassy and hard compared to the rubbery outer pBzA blocks. Again there is considerable opportunity to develop very novel new materials by combining cubes with ATRP methods.[73]

One other catalysis method, olefin metathesis, was examined briefly by Feher *et al*. In a short communication[76] it was mentioned that OVS could be reacted with a two-fold excess of styrene and/or 1-pentene in benzene in the presence of 6 mol% of a molybdenum metathesis (Schrock) catalyst under a slight vacuum (to remove generated ethene). This reaction, run at ambient, gave 70–100% conversions to the mostly *trans* products after 24 h. This approach to producing novel supramolecular materials has not been explored since, but deserves to be revisited because the reaction conditions are so mild and the potential to make novel nanobuilding blocks is so high.

A final hydrosilylation approach to introducing octafunctional building blocks for the synthesis of nanocomposites comes from the work of Matisons *et al*.[77] They were able to introduce isocyanate groups per reaction (11). The resulting product is a viscous oil that functions like a standard isocyanate and offers potential access to stars, dendrimers and a variety of nanocomposite materials, the subject of the next section.

Nancomposites

Above we briefly mention nanocomposites but here we begin with a formal discussion of one of the more important applications of cube nanobuilding blocks. The motivation for work done in this area is two-fold, one is based on concepts developed in the introduction, wherein the potential utility of cubes for designing materials nanometer by nanometer to provide optimal tailoring of global materials' properties is described. The other, also noted above, concerns the creation of materials where the volume fraction of interface is

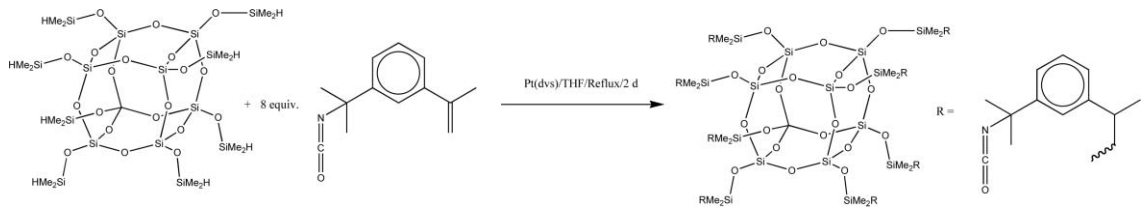

(11)

sufficiently high as to generate materials whose properties are nonlinearly related to the bulk properties of the components. These concepts were first described in a series of papers[78–83] summarized here.

The general idea is to create nanocomposites, schematically depicted in Fig. 11, that are constructed of hard and soft components such that the organization of the components is completely defined in terms of size, spatial relationships and with complete control of periodicity over macroscopic length scales. If the organic component or tethers that link the hard particles are short enough, then it is possible to create materials that are microporous (Fig. 11b). If the tethers are longer, then the pores between hard particles will be filled.

In principle, if the hard particles are all perfectly defined in dimensions, densities and chemical composition, then changes in global properties of any nanocomposites will be defined primarily by changes in the architecture or the organic tethers that link the hard particles. Given that OHS and OVS type compounds are completely defined in size ($\approx$1.2 nm diameter), are basically the equivalent of the smallest single crystal of silica, rigid, and offer the heat capacity (thermal robustness) of silica, they offer the best opportunity to develop nanocomposite materials wherein global properties can be tailored. In the following, we discuss their utility for making porous materials and epoxy resin nanocomposites.

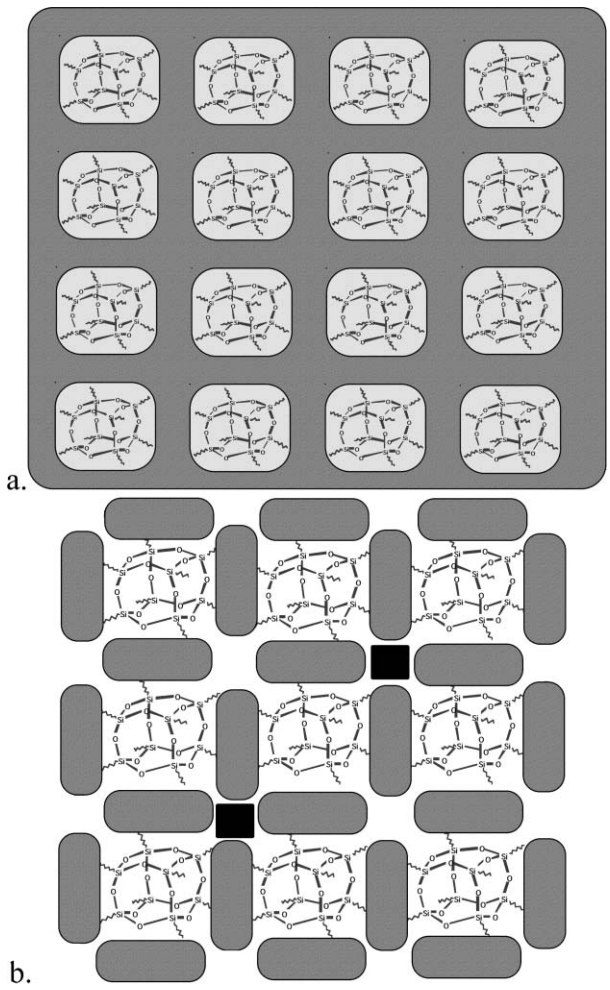

Fig. 11 Two nanocomposite morphologies: (a) continuous organic phase, (b) completely discontinuous nanocomposite with perfectly defined interfacial interactions and long-range periodicity at macroscopic length scales. Note potential for controlled microporosity symbolized in black.

Microporous materials

The reaction of the Si–H groups of OHS with the vinyl groups of OVS or its allyl analog provides the opportunity to produce micro- (7–20 Å) and mesoporous (20–500 Å) materials. Three groups have explored the use of Q_x species to produce porous materials beginning with the work of Hoebbel *et al.*[57,78,84–86] Harrison and Kannengiesser also describe using the related Q_6 compounds including $[BrMe_2SiOSiO_{1.5}]_6$, which they couple by hydrolysis.[85]

Two primary approaches were employed to form highly crosslinked porous materials based on the Q_x systems. In one approach the octaanion was reacted with dichlorosilanes or siloxanes to form crosslinks. However, the most facile approach reacts OHS with OVS, the allyl analog or with divinyl compounds[78,84] to produce gel-like systems that generate high surface area materials on drying. These materials do not appear to collapse from osmotic forces during solvent loss as is often experienced in sol–gel processing approaches to high surface area materials. A schematic of this process is given in Scheme 4.

Table 3 records data for a series of crosslinked systems including the OVS/OHS couple. These materials all exhibit relatively high surface areas given that no effort was made to supercritically dry them to produce aerogels. The pore volumes are not particularly high compared to typical aerogels but these materials can have such small pores that BET measurements (done with N_2) may not provide an accurate measure of the pore volume.

It is reasonable to assume that gelation will lead to high viscosities that in turn limit the extent of reaction. Furthermore, gelation coupled with the rigid cube structures might suggest that gelation will occur at very low crosslink densities as well. However, studies by solid state NMR indicate that the extents of reaction can be $>$80%.[78,84] This is equivalent to more than six bonds forming per cube for the coupling of OVS with OHS. Each cube has six faces suggesting a three dimensional, periodic structure.

One could attribute this high degree of reaction to the flexibility of the $OSiMe_2$ "spacers" that allow reorientation of cubes following initial reaction to form additional bonds. Another interpretation is that the catalyst species once sitting on one face of one cube zips all of the reactive groups on that face with a set of complementary functional groups on the face of another cube. One long-term implication here is that it may be possible to functionalize only one face at a time.

Support for a periodic 3-D structure comes from the pore size distribution for the OVS/OHS couple as shown in Fig. 12. Modeling studies suggest that the pore sizes that should form if the OVS/OHS couple reacts completely will be on average 1.2–1.5 nm (12–15 Å). As can be seen in Fig. 12, this is indeed the case. The majority of the pores are found in this region. The set of pores larger than 1.5 nm (15 Å) are explained by defects in

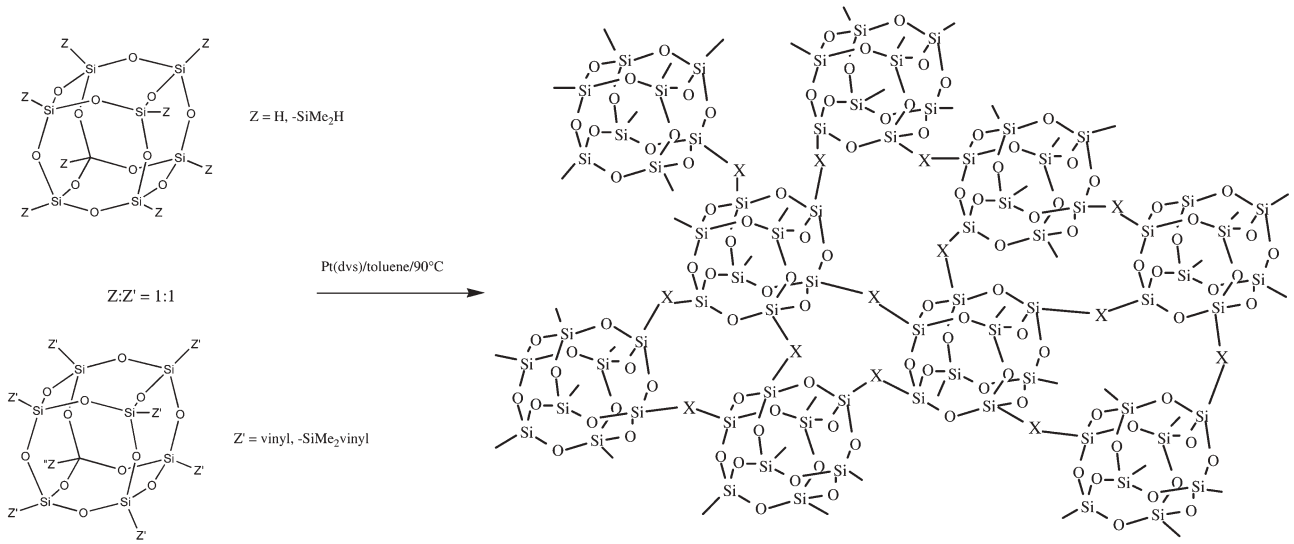

Scheme 4 Crosslinked polymers through hydrosilylation of oppositely functionalized cubes.[78]

Table 3 BET analyses (N_2 sorption) for a series of crosslinked cube systems from Scheme 4[78]

Polymer where X =	SSA/m^2 g^{-1}	Pore volume/ ml g^{-1}	% Reaction[a]
CH_2CH_2	529 ($\pm$43)	0.242 ($\pm$0.025)	45 $\pm$ 2
$OSiMe_2CH_2CH_2$	424 ($\pm$17)	0.191 ($\pm$0.015)	70 $\pm$ 2
$OSiMe_2CH_2CH_2SiMe_2O$	382 ($\pm$23)	0.203 ($\pm$0.026)	80 $\pm$ 2

[a] By solid state NMR.[78] Reflects degree of crosslinking.

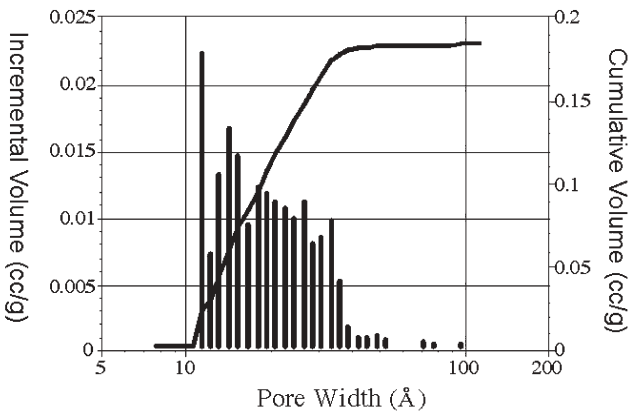

Fig. 12 Pore size distribution for 80% reaction of OVS with OHS.[78]

the nanocomposite where one or two cubes are missing. This accounts for all of the pores seen. The size, shape and number of the smaller pores as determined by BET were corroborated using positron annihilation lifetime spectroscopy.

Also of considerable importance is the fact that when the ''tethers'' between cube vertices are smaller and less flexible, the thermal stability increases. The Fig. 13 TGA of the OVS/OHS couple shows thermal stability in air to 300 °C. Such porous systems may offer low-*k* dielectric properties if the thermal stabilities can be increased to near 400 °C.[87,88]

The above results are similar to those reported by Harrison and Kannengiesser, and Hoebbel *et al.* with the exception that

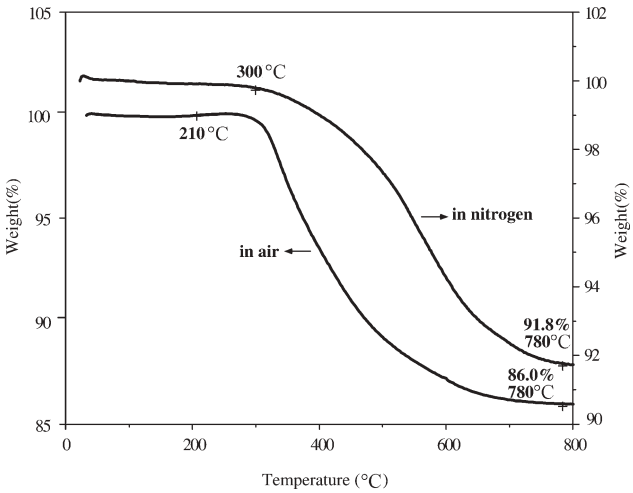

Fig. 13 TGA of OVS/OHS copolymer in air and nitrogen.

in Hoebbel *et al.*'s work, they report that as the chains linking the cubes become longer than about 7 atoms, the microporosity disappears.

In unpublished work,[89,90] we observe the same results. By converting OHS to a bifunctional cube with an average of four cyclohexenylethyl groups, reaction (12), we can create a self-curing compound, TCHS, that melts at 60 °C, and cures at >150 °C, reaction (13), to produce transparent materials that are now even more thermally stable in air, see Fig. 14.

We have commented above that the coupling of cubes should lead to long-range periodicities. Fig. 15 provides a comparison of the X-ray diffraction powder patterns for OHS, TCHS, the octafunctionalized analog, OCHS, and the polymer produced in reaction (13).

The XRD data are best described by using the OHS powder pattern as a reference point. Three primary peaks seen for OHS are at 8.3°, 18.9° and 24.4° 2θ indicating a crystalline material. Indeed, the crystal structure is known.[56] These peaks represent periodic distances of 1.1, 0.5 and 0.3 nm and are

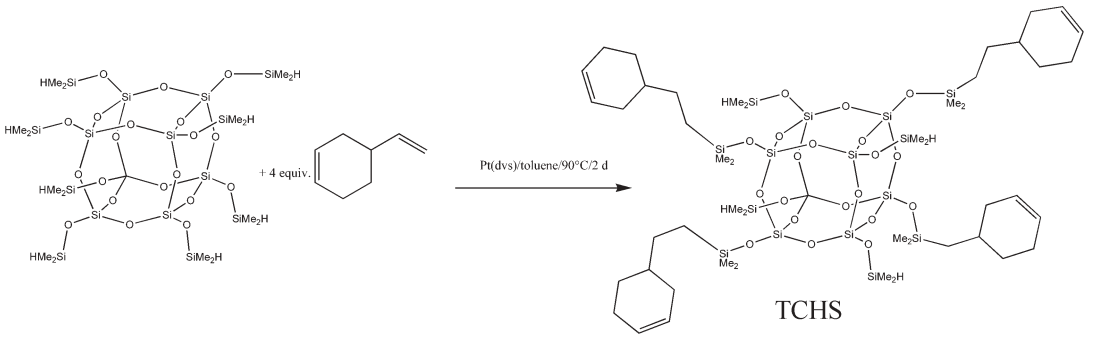

(12)

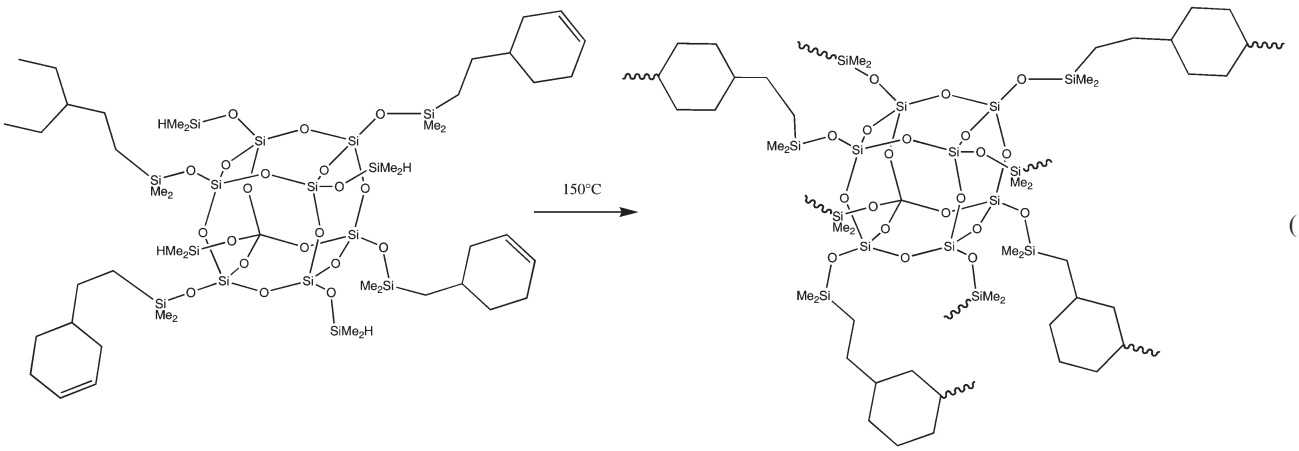

(13)

assigned to the (100) or (010), (120) and (112) planes, respectively. The 0.5 nm distance likely corresponds to the cube (core) body diagonal. The 0.3 nm peak likely corresponds to the separation between the 4–4′ rings of the cubes—the distance between cube faces.

One can interpret the data for TCHS and OCHS as follows. In these systems, the materials are only partially crystalline as suggested by the broad peak for TCHS at 7.3° 2θ, indicative of a larger unit cell (1.3–1.4 nm), as might be expected for an irregularly substituted cube. The peak at 18.9° 2θ shifts only slightly to 18.5° 2θ and does not exhibit any broadening suggesting a direct relationship to the core structure, as suggested above. Also, the peak at 24.4° 2θ disappears.

In the OCHS material, we see a similar pattern. The lowest peak shifts further to 6.5° 2θ indicating a slight but further increase in unit cell size. A similar shift to slightly lower angles gives a peak at 18.1° 2θ.

Finally, the crosslinked resin produced by thermal promotion of hydrosilylation also exhibits some ordering. TCHS resin (Fig. 14) magnified 5× reveals broad weak peaks centered at 7.5° and 17.5° 2θ suggesting some periodicity within the resin structure. The fact that these peaks are relatively close to the peak positions in TCHS suggests only

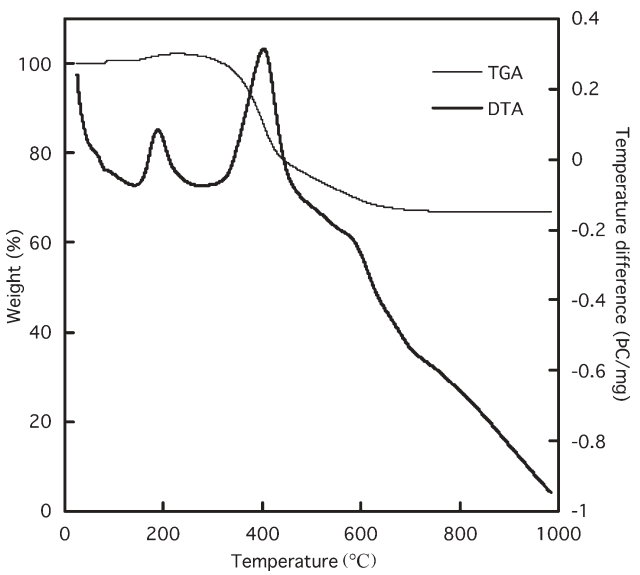

Fig. 14 TGA/DTA of TCHS in air, ramp rate 10 °C min^{-1}.

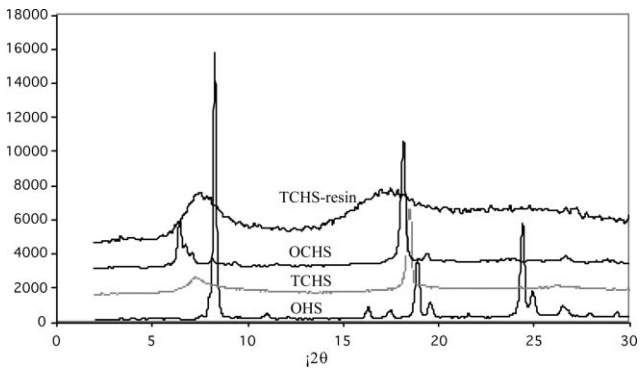

Fig. 15 XRD data for OHS, TCHS, OCHS, and thermal cured TCHS (×5).

modest changes in the cured structure. The fact that there is any order at all may be attributed to the flexibility of the resulting ethylcyclohexyl tethers which can be expected to allow at least some ordering in the almost fully crosslinked system. It is important to note that these systems are likely to be true 3-D networks given the random organization of the reacting groups.

Our original goal here was to create a system that would melt before self-curing thereby needing no solvents and that would also produce microporous materials. The idea behind this approach was to assume that the orthogonal functional groups could not react with each other and would be forced to react only with functional groups on other cubes. Indeed this does seem to happen but unfortunately, we find no evidence for microporosity.

Apparently, flexible bridges longer than 6 or 7 atoms also lead to nonporous materials in polymeric organic bridged silsesquioxanes as well.[14] The ability to create materials with exceptional control of periodicity as found for the above porous materials suggested that it should be possible to find chemistries that allow one to couple vertices on cubes such that each vertex is joined to only one other vertex. This led to studies on epoxy resins.

Epoxy based nanocomposites

The opportunity to make self-reinforced epoxy nanocomposites offers considerable potential from both academic and commercial perspectives. A number of groups have explored the use of Q_x derived epoxy systems for developing materials with novel properties.[7,79–83,91–93] From an academic point of view, octaepoxy resin systems offer the potential to test the concept of creating nanocomposites made using perfectly-defined hard particles modified with structurally related but dissimilar functional groups. If it is possible to generate materials with different global properties that can be proved to arise from these structural dissimilarities *i.e. via* modeling studies, then these results provide support for the concept of nanotailoring of macroscopic properties.

To this end, work in our group explored the reactions of the OG and OC cubes shown with a standard aromatic amine, diaminodiphenylmethane, DDM. The DDM/DGEBA couple was used as a standard resin. Mather *et al.* have conducted complementary studies using the sulfone equivalent of DDM.[7a]

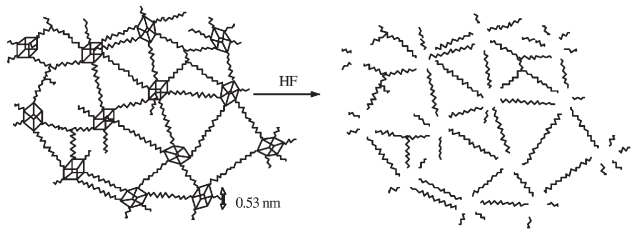

Fig. 16 HF dissolution of the silica cage in cube nanocomposites releases the crosslinks for analysis by gel permeation chromatography, GPC.

The key differences in the two epoxies, OG and OC, center on the addition of an extra carbon that forms the ring structure making OC less flexible than OG.

All of the epoxies were reacted with DDM at multiple ratios of epoxy to amine under conditions (150 °C/, 10 h) where essentially complete curing occurs. Based on epoxy resin curing chemistry, there are two stoichiometries that provide minimum defect structures. These occur when one epoxy reacts once with an NH_2 group or where two epoxy groups react with one NH_2. The reason that these are called minimum defect stoichiometries is that one assumes that as the reaction proceeds, the resin viscosity increases to the point where complete reaction is essentially impossible.

Three systems were compared; OG/DDM, OC/DDM and the commercial aircraft epoxy resin, DGEBA/DDM. First, OC/DDM and OG/DDM nanocomposites were characterized to establish the types of crosslinks that form. Dissolution of the silica cage out of these nanocomposites using HF, Fig. 16, followed by extraction of the residual organics and analysis by GPC (Fig. 17) indicates that as formed (1 : 1 stoichiometry for OC : DDM), at least 90% of the crosslinks are single links between cube vertices as suggested in Fig. 16.

These crosslinks must come from a species such as shown below:

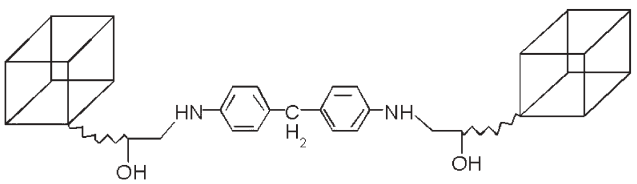

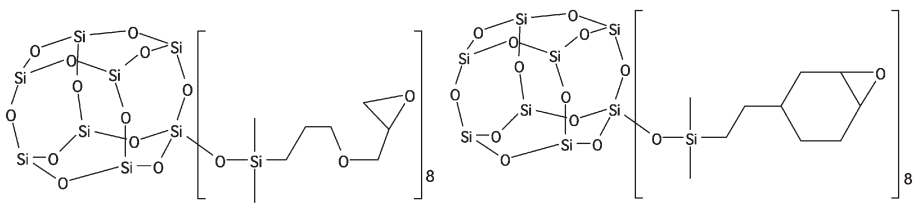

Octaglycidyl = OG

Octaethylcyclohexenyl epoxide = OC

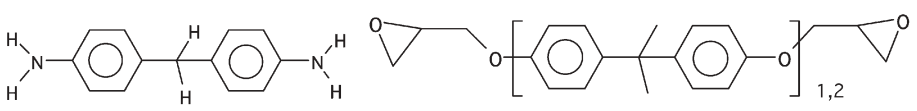

DDM

DGEBA

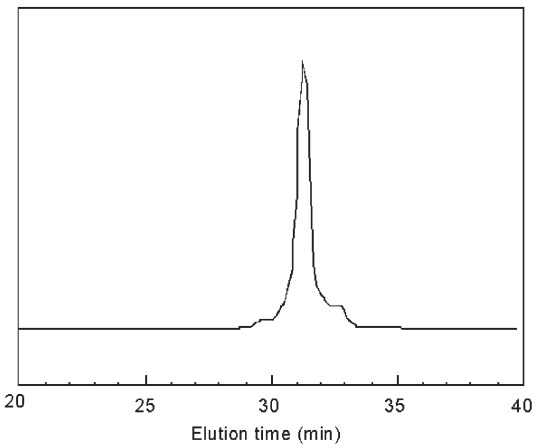

Fig. 17 GPC of extract from OC : DDM 1 : 1 nanocomposite following HF dissolution.[79] Data support the formation of mostly single tether structures joining two cube vertices.

The implication is that the nanocomposite is indeed primarily a completely discontinuous nanocomposite with only one organic species linking the hard particle. At the chemical level, the material is homogeneous and periodic over large length scales. The samples used here were cast tensile test specimens tens of mm in length. In contrast, the OG materials contained some 20% crosslinks that had double functionality on one nitrogen and none at other nitrogens, making them less uniform.[79]

Although chemical uniformity is a good beginning, it is still possible to have segregation at larger length scales. Thus, TEM studies of the same OC/DDM nanocomposite system were done as shown in Fig. 18.[81] From TEM studies, it is apparent that there is no segregation at nanometer length scales again suggesting excellent homogeneity at long length scales. Optical microscopy studies also showed no evidence of segregation at still longer length scales. Note these results contrast with those of Mather *et al.* as discussed below.[7]

Fig. 19 compares the mechanical properties (elastic moduli) of all three resins. Fig. 20 shows fracture toughness data in units of K_1C.[80,81] These epoxy resin composites differ

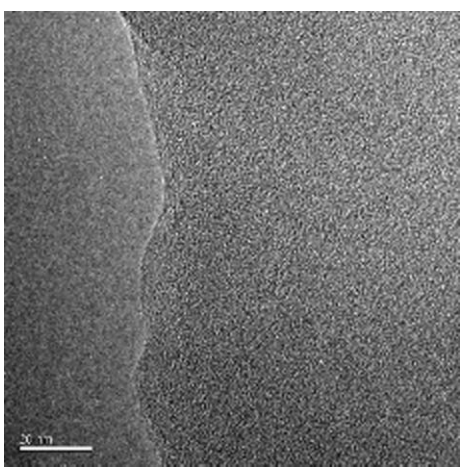

Fig. 18 TEM of OC : DDM at 1 : 1 stoichiometry (right side of image, scale bar is 20 nm).[81]

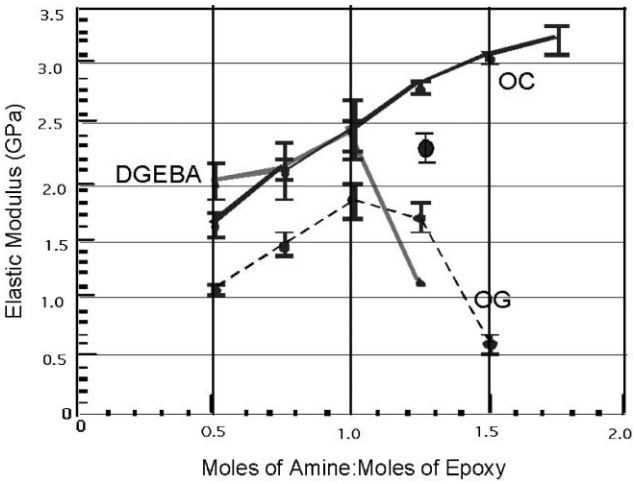

Fig. 19 Comparison of tensile strengths for OG/, OC/ with DGEBA/DDM composites at various amine : epoxy stoichiometries, N. Single point at $N = 1.25$ is for 70 : 30 OG : OC composite.

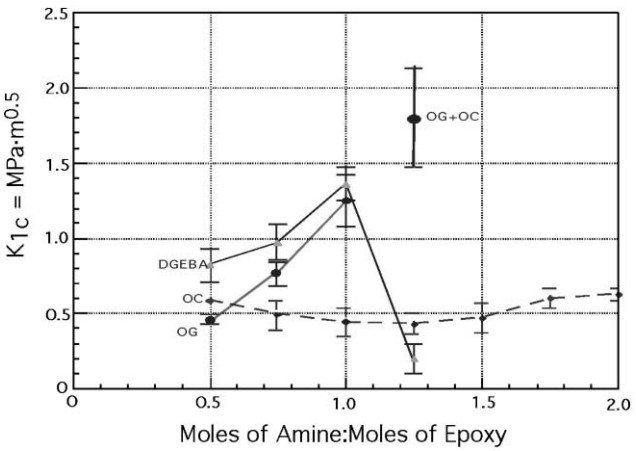

Fig. 20 Comparison of fracture toughness for OG/, OC/ with DGEBA/DDM composites at various amine : epoxy stoichiometries, N. Single point at $N = 1.25$ is for 70 : 30 OG : OC composite.

quite significantly. Note that $N = 0.5$, with two epoxy groups per NH_2, is the standard stoichiometry for commercial epoxy resins.

The change from an open chain flexible epoxy to a closed-ring epoxy on going from OG to OC results in very different properties. On comparing tensile strengths for all three systems, the commercial stoichiometry offers the best values until the stoichiometries shift to $N > 1.0$. Here a dichotomy develops.

At $N > 1.0$, the tensile strengths of the OG and DGEBA composites fall off as more and more defects are introduced. In contrast, the OC composites continue to increase in tensile strength as the number of defects grows to the last point tested. Indeed the tensile strength at 3.3 GPa is 100% greater than that of DGEBA/DDM at $N = 0.5$ where it is normally used. These values are quite impressive for an epoxy until one looks at the fracture toughness values, Fig. 20.

The fracture toughness data also show significant contrasts. The OG and DGEBA systems again follow normal behavior

with fracture toughness increasing from $N = 0.5$ to 1.0. For OC, there is no major change in behavior over every composition tested. This significant difference in behavior is important because, in principle, it suggests that one can tailor properties at nanometer length scales. If true, then modeling studies could be used to understand how the architecture of the organic component between the hard particles controls the global mechanical properties.

Theoretical studies on ''simplified'' two tether links between two cubes permit modeling of the behavior of the epoxy ''tether'' components. Fig. 21 models the stretching behavior of the tethers. The flexibility of the OG system is such that its point of closest approach, 1.7 nm, is almost half the distance of the point of farthest separation. In contrast, in the OC system, the point of closest approach is 1.3 nm and the point of farthest separation is only 1.9 nm, almost the equivalent to the closest approach in the OG system. The OC tether has very limited flexibility.

Most important, it is possible to directly relate this behavior to the global mechanical properties. The OG system shows poor tensile strength because the tether system clearly is sufficiently elastic to deform plastically (as seen[80,81]) rather than resist elongation. Likewise, bend strengths reflect the easy deformation of the OG tethers such that these materials plastically deform much more readily than the OC system. The OC behavior comes from a combination of: (1) limited opportunity for tethers to plastically deform, and (2) the coiled structure and limited flexibility of the OC tether, which in turn suggests that these bonds are at a much higher energy than for the OG structures, as discussed in the original reports.[80,81]

Thus, it appears that it is possible to control and even predict global properties by understanding the effects of changes in the architectures of the organic components between cubes. This is providing one is able to obtain a high degree of reactivity so that one obtains uniform materials over long length scales.

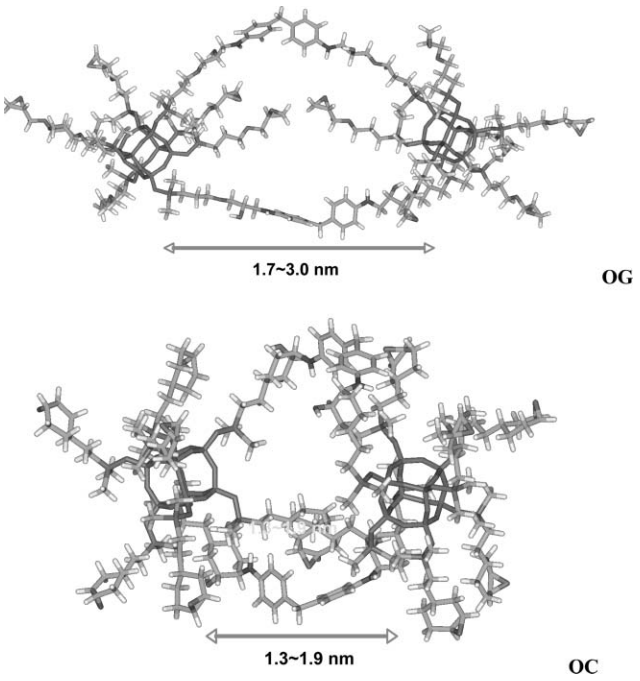

Fig. 21 Modeling of the stretching behavior of the tethers in OG/DGEBA and OC/DGEBA nanocomposite systems.[76]

It is important to recognize that even simple modifications can lead to quite different behaviors. Mather *et al.*[7a] have studied the same types of nanocomposites formulated by reacting OG with DDS using very similar processing methods. They find that, depending on the overall ratio of DDS to OG, there can be extensive aggregation of the OG units. This aggregation was found to diminish with increasing amounts of DDS but even under optimal conditions, persistent aggregates exist in the 12–15 nm size range. Furthermore, they find that the mechanical properties of these materials are affected by the presence of these aggregates.

In elegant TEM studies, they were able to identify what appear to be the principle failure mechanisms for these types of nanocomposites. They find, by imaging in near-crack regions, deformation arises because these aggregates cause localized shear deformation with subsequent plastic growth of voids in the epoxy matrix. The result is diffuse shear yielding, which when combined with large concentrations of small local plastic deformation events actually provides a mechanism for absorbing large amounts of strain energy, which for OG translates to toughening of brittle or notch sensitive materials. The most likely explanation for the formation of aggregates comes from the DDS reacting to form branched or bifurcated tethers[80,81] between as many as four different cubes per single DDS. This is in keeping with the observation that the degree of aggregation decreases as the amounts of DDS relative to OG increase. This is also in keeping with our observations that even at $N = 1.0$, up to 20% of the DDM forms bifurcated tethers. In contrast, OC is sterically prevented from reacting a second time with a DDM nitrogen. Hence, aggregation by formation of bifurcated tethers is prevented and these nanocomposites exhibit essentially complete discontinuity.

Given that it appears possible to tailor the global properties of these nanocomposites, mixed 75OG+25OC/DDM nanocomposites were made (see Figs. 19 and 20) using an $N = 1.25$ value, where OG and DGEBA nanocomposites fair very poorly. The resulting materials offer K_1C (fracture toughness) values of 2.5 (*vs.* 0.8 for DGEBA/DDM) and elastic moduli of 2.4 GPa (comparable to DGEBA/DDM at $N = 1$) well above any of those observed in the simple systems discussed above. Thus, tailoring can be done in these systems once an understanding of the mechanics of behavior of the organic architecture is available.

One final note on epoxy resins: the results found here suggest that optimal mechanical properties occur at epoxy resin stoichiometries of $N = 1$ rather than $N = 0.5$. As we will show in other papers, this stoichiometry provides excellent opportunities to control the CTE (coefficient of thermal expansion) of epoxy resins for some applications. However, there are complications with the fact that in some systems the $N = 1$ stoichiometry gives linear segments that lower the resin T_g too much. In other systems, the moisture susceptibility resulting from unreacted N–H groups can be too high. However, in Q_8 systems which have $OSiMe_2$ units, moisture susceptibility is relatively low, *e.g.* 0.5 wt% pickup for 7 days immersion in water for the $N = 1.0$ OC/DDM materials.

The future

The above discussions and data suggest that it is indeed possible to use octafunctional cubes to build structures nanometer by nanometer with good-to-excellent control of the architecture at multiple length scales. The use of the Q_6 and Q_{10} species as nanobuilding blocks has barely been explored. Cubes offer potential access to numerous nanostructures for a wide variety of applications including the development of:

- core–shell architectures,
- dendrimers and hyperbranched materials,
- Janus (two faced) particles
- porous materials for
  - ○ low-*k* dielectrics
  - ○ encapsulants for drug delivery
  - ○ confined space catalytic studies
  - ○ hydrogen storage
  - ○ gas and liquid separations
  - ○ pollutant trapping
  - ○ analytical applications (*e.g.* for column chromatography, concentrators, *etc.*)
- highly polyfunctional materials
- novel functional coatings systems.

This list is by no means complete and is intended solely to inspire others to explore the many unique compounds and materials that can be made simply and at low cost from just about any silica source.

Acknowledgements

The author would like to thank the many colleagues and collaborators that helped conduct much of the research described above. In particular, Professor Isao Hasegawa is thanked for a careful and critical reading of this review. Support for the research came from many sources including the National Institutes of Dental Research, The Federal Aviation Administration, The Air Force Office of Scientific Research, NSF (IGERT), The Office of Naval Research, ESPE Dental-Medizin (Now 3 M) Canon Research America, Matsushita Electric Ltd., Delphi Inc., Kuraray Ltd, Guardian Industries, Nippon Shokubai Ltd., and Mayaterials Inc.

Figs. 1, 8, 9, 12, 13, 16–19 and Schemes 1, 2, 4 are reprinted from the references cited by permission from the American Chemical Society. Fig. 20 is reprinted by permission from Advanced Materials.

References

1 (*a*) F. J. Feher, D. A. Newman and J. F. Walzer, Silsesquioxanes as models for silica surfaces, *J. Am. Chem. Soc.*, 1989, **111**, 1741; (*b*) F. J. Feher, T. A. Budzichowski, R. L. Blanski, K. J. Weller and J. W. Ziller, Facile syntheses of new incompletely condensed polyhedral oligosilsesquioxanes: $[(c\text{-}C_5H_9)_7Si_7O_9(OH)_3]$, $[(c\text{-}C_7H_{13})_7Si_7O_9(OH)_3]$, and $[(c\text{-}C_7H_{13})_6Si_6O_7(OH)_4]$, *Organometallics*, 1991, **10**, 2526; (*c*) F. J. Feher, D. Soulivong, A. G. Eklud and K. D. Wyndham, Cross-metathesis of alkenes with vinyl-substituted silsesquioxanes and spherosilicates: a new method for synthesizing highly-functionalized Si/O frameworks, *Chem. Commun.*, 1997, 1185.

2 (*a*) F. J. Feher and R. L. Blanski, Olefin polymerization by vanadium-containing silsesquioxanes: synthesis of a dialkyl-oxo-vanadium(V) complex that initiates ethylene polymerization, *J. Am. Chem. Soc.*, 1992, **114**, 5886; (*b*) J. R. Severn, R. Duchateau, R. A. van Santen, D. D. Ellis and A. L. Spek, Homogeneous Models for Chemically Tethered Silica-Supported Olefin Polymerization Catalysts, *Organometallics*, 2002, **1**, 4; (*c*) R. Duchateau, H. C. L. Abbenhuis, R. A. van Santen, A. Meetsma, S. K.-H. Thiele and M. F. H. van Tol, Ethylene Polymerization with Dimeric Zirconium and Hafnium Silsesquioxane Complexes, *Organometallics*, 1998, **26**, 5663; (*d*) R. W. J. M. Hanssen, R. A. van Santen and H. C. L. Abbenjuis, Dynamic Status Quo of Polyhedral Silsesquioxane Coordination Chemistry, *Eur. J. Inorg. Chem.*, 2004, 675–683.

3 N. Maxim, P. C. M. M. Magusin, P. J. Kooyman, J. H. M. C. van Wolput, R. A. van Santen and H. C. L. Abbenhuis, Microporous Mg-Si-O and Al-Si-O Materials Derived from Metal Silsesquioxanes, *Chem. Mater.*, 2001, **13**, 2958.

4 C. Bonhomme, P. Toledano, J. Maquet, J. Livage and L. Bohnomme-Coury, Studies of octameric vinylsilasesquioxane by carbon-13 and silicon-29 cross polarization magic angle spinning and inversion recovery cross polarization nuclear magnetic resonance spectroscopy, *J. Chem. Soc., Dalton Trans.*, 1997, 1617.

5 (*a*) A. R. Bassindale, M. Pourny, P. G. Taylor, M. B. Hursthouse and M. E. Light, Fluoride-Ion Encapsulation within a Silsesquioxane Cage, *Angew. Chem., Int. Ed.*, 2003, **42**, 3488; (*b*) A. R. Bassindale, D. J. Parker, M. Pourny, P. G. Taylor, P. N. Horton and M. B. Hursthouse, Fluoride Ion Entrapment in Octasilsesquioxane Cages as Models for Ion Entrapment in Zeolites. Further Examples, X-ray Crystal Structure Studies, and Investigations into How and Why They May Be Formed, *Organometallics*, 2004, **23**, 4400.

6 A. Tsuchida, C. Bollin, F. G. Sernetz, H. Frey and R. Mülhaupt, Microporous Mg-Si-O and Al-Si-O Materials Derived from Metal Silsesquioxanes, *Macromolecules*, 1997, **30**, 2818.

7 (*a*) G.-M. Kim, H. Qin, X. Fang, F. C. Sun and P. T. Mather, Hybrid Epoxy-Based Thermosets Based on Polyhedral Oligosilsesquioxanes: Cure Behavior and Toughening Mechanisms, *J. Polym. Sci. B: Polym. Phys.*, 2003, **41**, 3299–3313; (*b*) B. S. Kim and P. T. Mather, Amphiphilic telechelics incorporating polyhedral oligosilsesquioxane: 1. Synthesis and characterization, *Macromolecules*, 2002, **35**, 8378–8384; (*c*) R. I. Gonzalez, S. H. Phillips and G. B. Hoflund, *J. Spacecraft Rockets*, 2000, **37**, 463.

8 (*a*) A. J. Waddon and E. B. Coughlin, Crystal structure of polyhedral oligomeric silsequioxane (POSS) nano-materials: A study by X-ray diffraction and electron microscopy, *Chem. Mater.*, 2003, **15**, 4555–4561; (*b*) G. Cardoen and E. B. Coughlin, Hemitelechelic polystyrene-POSS copolymers as model systems for the study of well-defined inorganic/organic hybrid materials, *Macromolecules*, 2004, **37**, 5123–5126.

9 (*a*) B. X. Fu, B. S. Hsiao, H. White, M. Rafailovich, P. Mather, H. G. Joen, S. Phillips, J. Lichtenhan and J. Schwab, Nanoscale Reinforcement of Polyhedral Oligomeric Silsesquioxane (POSS) in Polyurethane Elastomer, *Polym. Int.*, 2000, **49**, 437–440; (*b*) B. X. Fu, W. Zhang, B. S. Hsiao, M. Rafailovich, J. Sokolov, G. Johansson, B. B. Sauer, S. Phillips and R. Blanski, Synthesis and Characterization of Segmented Polyurethane Containing Polyhedral Oligomeric Silsesquioxane (POSS) Nanostructured Molecules, *High Performance Polym.*, 2001, **12**, 565–571.

10 (*a*) E. S. Baker, J. Gidden, S. E. Anderson, T. S. Haddad and M. T. Bowers, Isomeric Structural Characterization of Polyhedral Oligomeric Silsesquioxanes (POSS) with Styryl and Epoxy Phenyl Capping Agents, *Nano Lett.*, 2004, **4**, 779–785; (*b*) B. X. Fu, A. Lee and T. S. Haddad, Styrene–Butadiene–Styrene Triblock Copolymers Modified with Polyhedral Oligomeric Silsesquioxanes, *Macromolecules*, 2004, **37**, 5211–5218; (*c*) E. T. Kopesky, T. S. Haddad, R. E. Cohen and G. H. McKinley, Thermomechanical Properties of Poly(methyl methacrylate)s Containing Tethered and Untethered Polyhedral Oligomeric Silsesquioxanes, *Macromolecules*, 2004, **37**, 8992–9004.

11 M. G. Voronkov and V. I. Lavrent'yev, Polyhedral Oligosilsesquioxanes and Their Homo Derivatives, *Top. Curr. Chem.*, 1982, **102**, 199–236.

12 R. H. Baney, M. Itoh, A. Sakakibara and T. Suzuki, Silsesquioxanes, *Chem. Rev.*, 1995, **95**, 1409–1430.

13 A. Provatas and J. G. Matisons, Synthesis and applications of silsesquioxanes, *Trends Polym. Sci.*, 1997, **5**, 327–333.

14 D. A. Loy and K. J. Shea, Bridged Polysilsesquioxanes. Highly Porous Hybrid Organic–Inorganic Materials, *Chem. Rev.*, 1995, **95**, 1431–1442.

15 J. Lichtenhan, Silsesquioxane-based Polymers, in *Polymeric Materials Encyclopedia*, ed. J. C. Salmone, CRC Press, NY, 1996, vol. 10, pp. 7768–7777.

16 (*a*) D. Hoebbel and W. Wieker, Die Konstitution des Tetramethylammoniumsilicats der Zusammensetzung 1,0 $N(CH_3)_4OH$ 1,0 SiO_2·8,0–8,3 H_2O, *Z. Anorg. Allg. Chem.*, 1971, **384**, 43–52; (*b*) Yu. I. Smolin, *Sov. Phys. Crystallogr.*, 1970, **15**, 23–25.

17 D. Hoebbel, W. Wieker, P. Franke and A. Otto, Zur Konstitution des neuen Silicatanions $[Si_{10}O_{25}]_{10}^-$, *Z. Anorg. Allg. Chem*, 1975, **418**, 35–44.

18 I. Hasegawa and S. Sakka, Silicate Species with Cagelike Structure in Solutions and Rapid Solidification with Organic Quaternary Ammonium Ions, in *Zeolite Synthesis*, ACS Symp. Ser. 398, ed. M. L. Occelli and H. E. Robson, American Chemical Society, Washington, DC, 1989, pp. 140–151.

19 D. Hoebbel, G. Garzó, G. Engelhardt, R. Ebert, E. Lippmaa and M. Alla, Über, die Silicatanionenkonstitution in Tetraethylammoniumsilicaten und ihren wäßrigen Lösungen, *Z. Anorg. Allg. Chem*, 1975, **465**, 15–33. First report of the hexasilicate.

20 R. K. Harris and C. T. G. Knight, Silicon-29 NMR Studies of Aqueous Silicate Solutions, Part IV. Tetraalkylammonium hydroxide solutions, *J. Mol. Struct.*, 1982, **78**, 273–8.

21 D. Hoebbel, A. Vargha, G. Engelhardt and K. Ujszászy, Zum Anionenaufbau von Tetra-n-butylammoniumsilicaten und ihren wäßrigen Lösungen, *Z. Anorg. Allg. Chem*, 1984, **509**, 85–94. nBu_4N at low 0.8–1.0 concentrations gives deca, at higher than 1 : 0.4 six forms.

22 R. Stodolski, D. Heidemann, W. Wieker and W. Pilz, Thermische Zersetzung von Afwillit $Ca_3(SiO_3OH)_2$·2 H_2O, *Z. Anorg. Allg. Chem*, 1985, **527**, 150–160. Concentrated TEAmmonium gives hexa whereas tetrapropyl gives a broad distribution of ions.

23 F. Schlenkrich, O. Rademacher and H. Scheler, Vergleichende Untersuchungen zur Silicationenkonstitution in $[(Ethyl)_n(2\text{-hydroxyethyl})_{4-n}$ammonium]-Silicatlösungen mit n von 3 bis 1 und zum Einfluß von Alkalihydroxid, *Z. Anorg. Allg. Chem.*, 1987, **547**, 109–117. Where $N = 1$ to 3, at higher choline more OSA, with some alkali destroys the equilibria.

24 I. Hasegawa, S. Sakka, K. Kuroda and C. Kato, The Effect of Tetramethylammonium Ions on the Distribution of Silicate Species in the Methanolic Solutions, *J. Mol. Liq.*, 1987, **34**, 307–315.

25 I. Hasegawa, S. Sakka, K. Kuroda and C. Kato, The Effect of Sodium Ions on the Distribution of Silicate Anions in Tetramethylammonium Silicate Aqueous Solutions, *Bull. Inst. Chem. Res. Kyoto Univ.*, 1987, **65**, 5–6.

26 I. Hasegawa and S. Sakka, Rapid Solidification of (2-Hydroxyethyl)trimethylammonium Silicate, *Chem. Lett.*, 1988, 1319–1322.

27 F. Schlenkrich, O. Rademacher and H. Scheler, On the Silicate Constitution in mixtures of tetraethylammonium-triethyl-(2-hydroxyethyl)ammonium silicate solutions and triethyl-(2-hydroxypropyl)ammonium - triethyl-(2-hydroxyethyl)ammonium silicate solutions. Formation of crystalline double-ring silicate hydrates, *Z. Anorg. Allg. Chem*, 1990, **582**, 169–178. Concentration of D4R increases with ratios closer to 1 : 1 N : Si.

28 R. K. Harris, C. T. G. Knight and W. E. Hull, Nature of Species Present in Aqueous Potassium Silicate Solutions, *J. Am. Chem. Soc.*, 1981, **103**, 1577–1578.

29 (*a*) A. Firouzi, F. Atef, A. G. Oertli, G. D. Stucky and B. F. Chmelka, Alkaline Lyotropic Silicate-Surfactant Liquid Crystals, *J. Am. Chem. Soc.*, 1997, **119**, 9466–9477; (*b*) A. Firouzi, D. J. Schaefer, S. H. Tolbert, G. D. Stucky and B. F. Chmelka, Magnetic-Field-Induced Orientational Ordering of Alkaline Lyotropic Silicate-Surfactant Crystals, *J. Am. Chem. Soc.*, 1997, **119**, 9466–9477 and references therein.

30 C. T. G. Knight, Are zeolite secondary building units really red herrings?, *Zeolite*, 1990, **10**, 140–144.

31 R. M. Laine, K. Y. Blohowiak, T. R. Robinson, M. L. Hoppe, P. Nardi, J. Kampf and J. Uhm, Synthesis of Novel, Pentacoordinate Silicon Complexes from SiO_2, *Nature*, 1991, **353**, 642–644.

32 H. Cheng, R. Tamaki, R. M. Laine, F. Babonneau, Y. Chujo and D. R. Treadwell, Neutral Alkoxysilanes from Silica, *J. Am. Chem. Soc.*, 2000, **122**, 10063–10072.

33 M. Z. Asuncion, I. Hasegawa, J. Kampf and R. M. Laine, The selective dissolution of rice hull ash to form $[OSiO_{1.5}]_8[R_4N]_8$ (R = Me, CH_2CH_2OH) octasilicates. Basic nanobuilding blocks and possible models of intermediates formed during biosilification processes, *J. Mater. Chem.*, 2005, **15**, 2114–2121.

34 T. Kudo and M. Gordon, Exploring the Mechanism for the Synthesis of Silsesquioxanes. 3. The Effect of Substituents and Water, *J. Phys. Chem. A*, 2002, **106**, 11347–11353.

35 T. Kudo and M. Gordon, Exploring the Mechanism for the Synthesis of Silsesquioxanes. 2. Cyclosiloxanes (D_3 and D_4), *J. Phys. Chem. A*, 2000, **104**, 4058–4063.

36 T. Kudo and M. Gordon, Theoretical Studies of the Mechanism for the Synthesis of Silsesquioxanes. 1. Hydrolysis and Initial Condensation, *J. Am. Chem. Soc.*, 1998, **120**, 11432–11438.

37 C. C. Perry and T. Keeling Tucker, Biosilicification: the role of the organic matrix in structure control, *J. Biol. Inorg. Chem.*, 2000, **5**, 537–550.

38 V. Martin-Jesequel, M. Hildebrand and M. A. Brzezinski, Silicon metabolism in diatoms: implications for growth, *J. Phycol.*, 2000, **36**, 821–840.

39 J. N. Cha, G. D. Stucky, D. E. Morse and T. J. Deming, Biomimetic synthesis of ordered silica structures mediated by block copolypeptides, *Nature*, 2000, **403**, 289–292.

40 Y. Zhou, K. Shimizu, J. N. Cha, G. D. Stucky and D. E. Morse, Efficient Catalysis of Polysiloxane Synthesis by Silicatein a Requires Specific Hydroxy and Imidazaole Functionalities, *Angew. Chem., Int. Ed.*, 1999, **38**, 781–782.

41 (*a*) N. Kröger, R. Duetzmann and M. Sumper, Polycationic Peptides from Diatom Biosiica That Direct Silica Nanosphere Formation, *Science*, 1999, **286**, 1129–1132; (*b*) N. Kröger, R. Duetzmann and M. Sumper, The Chemical Structure of Silaffin-1-A From Cylindrotheca Fuiformis, *J. Biol. Chem.*, 2001, **276**, 26066–26070.

42 (*a*) N. Kröger, S. Lorenz, E. Brunner and M. Sumper, Self-Assembly of Highly Phosphorylated Silafins and Their Function in Biosilica Morphogenesis, *Science*, 2002, **298**, 585–586; (*b*) S. Wenzl, R. Deutzmann, R. Hett, E. Hochmuth and M. Sumper, Quaternary Ammonium Groups in Silica-Associated Proteins, *Angew. Chem.*, 2004, **116**, 6059–6062.

43 C. C. Perry and S. Mann, Aspects of Biosilification, in *Origin, Evolution and Modern Aspects of Biomineralization in Plants and Animals*, ed. R. E. Crick, Plenum Press, New York, 1989, pp. 419–431.

44 N. Sahai, Calculation of ^{29}Si NMR shifts of silicate complexes with carbohydrates, amino acids, and Multicarboxylic acids; Potential role in biological silica utilization, *Geochim. Cosmochim. Acta*, 2004, **68**, 227–237 and references therein.

45 M. Wiebcke, J. Emmer and J. Felsche, Structural links between zeolite-type and clathrate hydrate-type materials: strands of small clusters of water molecules interconnect oligomeric silicate $[Si_8O_{18}(OH)_2]^{6-}$ anions to generate the 3D host structure of the heteronetwork clathrate $[DMPI]_6[Si_8O_{18}(OH)_2]$·48.5$H_2O$ (DMPI = 1,1-dimethylpiperidinium), *J. Chem. Soc., Chem. Commun.*, 1993, 1604–1605.

46 G. Bissert and F. Liebau, Crystal structure of $[N(n\text{-}C_4H_9)_4]H_7$-$[Si_8O_{20}]$·5.33$H_2O$ a zeolite A-like double ring silicate with protonated water clusters $[H_{41}O_{16}]^{9+}$, *Z. Kristallogr.*, 1987, **179**, 357–371.

47 J. Parkinson and R. Gordon, Beyond Micromachining: the Potential of Diatoms, *Trends Biotechnol.*, 1999, **17**, 190–196.

48 C. W. Lentz, Silicate Minerals as Sources of Trimethylsilyl Silicates and Silicate Structure Analysis of Sodium Silicate Solutions, *Inorg. Chem.*, 1964, **3**, 574–579.

49 P. A. Agaskar, Facile, High-Yield Synthesis of Functionalized Spherosilicates: Precursors of Novel Organolithic Macromolecular Materials, *Inorg. Chem.*, 1990, **29**, 1603.

50 D. Hoebbel, I. Pitsch, T. Reiher, W. Hiller, H. Jancke and D. Müller, Synthese, Aufbau und Eigenscaftern käfigartiger vinyl- und allylsilylieter Kieselsäuren, *Z. Anorg. Allg. Chem.*, 1989, **576**, 160–168.

51 D. Hoebbel, I. Pitsch, H. Wolf, S. Dathe, E. Popowski, G. Sonnek, T. Reiher, H. Janacke and U. Schelm, Organophile Doppelringkieselsäurederivate mit käfigartigen Structure, Verfahren zu Ihrer Herstellung und Ihre Verwendung, *Eur. Pat.*, EP 0 348 705 A2, Aug. 1989.

52 (*a*) R. Weidner, N. Zeller, B. Deubzer and V. Frey, Organooligosilsesquioxanes, *US Pat.*, 5,047,492, Sept. 1991; (*b*) R. Weidner, N. Zeller, B. Deubzer and V. Frey, Neue Organooligosilsesquioxanes, *Ger. Pat.*, 3837397, Oct. 1990.
53 C. Freyer and J. Wolferseder and U. Peetz, Organosiliciumverindungen mit käfigartiger Structur, *Eur. Pat.*, 0 624 591 A1, Nov. 1994.
54 D. Hoebbel, C. Weber, H. Schmidt and R.-P. Krüger, Synthesis and Properties of Perfluoroalkyl Groups Containing Double Four-Ring Spherosilicate (Siloxysilsesquioxane) Precursors, *J. Sol–Gel Sci. Technol.*, 2002, **24**, 121–129.
55 P. G. Harrison, R. Kannengiesser and C. J. Hall, High Yield Routes to Hexa(dimethylsilyloxy)-silsesquioxane and Hexa(bromodimethylsilyloxy)silsesquioxane, *Main Group Met. Chem.*, 1997, **20**, 137–140.
56 N. Auner, B. Ziemer, B. Herrschaft, W. Ziche, P. John and J. Weiss, Structural Studies of Novel Siloxysilsesquioxanes, *Eur. J. Inorg. Chem.*, 1999, 1087–1094.
57 D. Hoebbel, K. Endres, T. Reinert and I. Pitsch, Inorganic–organic polymers derived from functional silicic acid derivatives by additive reaction, *J. Non-Cryst. Solids*, 1994, **176**, 179–188.
58 F.-H. Kreuzer, R. Maurer and P. Spes, Liquid-Crystalline Silsesquioxanes, *Makromol. Chem. Macromol. Symp.*, 1991, **50**, 215–228.
59 G. H. Mehl and J. W. Goodby, Liquid-Crystalline, Substituted Octakis(dimethylsiloxy)octasil-sesquioxanes: Oligomeric Supermolecular Materials with Defined Topology, *Angew. Chem.*, 1996, **35**, 2641–2643.
60 I. M. Saez and J. W. Goodby, Supermolecular liquid crystal dendrimers based on the octasilsesquioxane core, *Liq. Cryst*, 1999, **26**, 1101–1105.
61 A. Sellinger, R. M. Laine, V. Chu and C. Viney, Palladium and Platinum Catalyzed Coupling Reactions of Allyloxy Aromatics with Hydridosilanes and Hydridosiloxanes: Novel Liquid Crystalline/Organosilane Materials, *J. Polym. Sci. Part A: Polym. Chem.*, 1994, **32**, 3069–3089.
62 C. Zhang, T. J. Bunning and R. M. Laine, Synthesis and Characterization of Liquid Crystalline (LC) Silsesquioxanes, *Chem. Mater.*, 2001, **13**, 3653–3662.
63 C. Zhang, Synthesis and Characterization of Octasilsesquioxane Based Molecular Composite Precursors with Potential Applications as Dental Restoratives, Ph.D. Dissertation, University of Michigan, 1999.
64 I. Hasegawa, T. Niwa and T. Takayama, Substitution of the dimethylsilyl group in $Si_8O_{20}[Si(CH_3)_2H]_8$ for another silyl group, *Inorg. Chem. Commun.*, 2005, **8**, 159–161.
65 P. Jutzi, C. Batz and A. Mutluay, Eightfold Functionalization of the Octasilsesquioxane Core, *Verlag Z. Naturforsch.*, 1994, 1689.
66 See for example J. F. Valliant, O. O. Sogbein, P. Morel, P. Schaffer, K. J. Guenther and A. D. Bain, Synthesis, NMR, and X-ray Crystallographic Analysis of C-Hydrazino-C-Carboxycarboranes: Versatile Ligands for the Preparation of BNCT and BNCS Agents and 99 mTc Radiopharmaceuticals, *Inorg. Chem.*, 2002, **41**, 2731–2737.
67 G. E. Southard and M. D. Curtis, Synthesis and Characterization of Soluble Poly(ferrocenyl-enearylene)s from Condensation of Dilithio Bis(alkylcyclopentadienide)arenes with Iron(II) Halides: A General Route to Conjugated Poly(metallocene)s, *Organometallics*, 2001, **20**, 508–522 and references therein.
68 M. Moran, C. M. Casado, I. Cuadrado and J. Losada, Ferrocenyl Substituted Octakis(di-methylsiloxy)octasilsesquioxanes: A New Class of Surpamolecular Organometallic Compounds. Synthesis, Characterization, and Electrochemistry, *Organometallics*, 1993, **12**, 4327–4333.
69 A. Sellinger and R. M. Laine, Silsesquioxanes as Synthetic Platforms. Thermally and Photo Curable Inorganic/Organic Hybrids, *Macromolecules*, 1996, **29**, 2327–2330.
70 C. Zhang and R. M. Laine, Hydrosilylation of allyl alcohol with $[HSiMe_2OSiO1.5]_8$. Octa (3-hydroxypropyldimethylsiloxy)octasilsesquioxane and its octamethacrylate derivative as potential precursors to hybrid nanocomposites, *J. Am. Chem. Soc.*, 2000, **122**, 6979–6988.
71 O. Toepfer, D. Neumann, N. R. Choudhury, A. Whittaker and J. Matisons, Organic–Inorganic Poly(Methyl Methacrylate) Hybrids with Confined Polyhedral Oligosilsesquioxane Macromonomers, *Chem. Mater.*, 2005, **17**, 1027–1035.
72 I. Hasegawa, R. M. Laine, M. Asuncion and N. Takamura, Facile Synthesis of the Cubeoctameric Silicate Anion, $Si_8O_{20}^{8-}$, its dimethylsilyl derivative, $Si_8O_{20}[Si(CH_3)_2H]_8$ and certain derivatives therefrom, *US Patent 2005/0142054*, June 30, 2005.
73 *Advances in Controlled/Living Radical Polymerization*, ed. K. Matyjaszewski, ACS, Washington DC, (distributed by Oxford University Press), 2003.
74 R. O. R. Costa, W. L. Vasconcelos, R. Tamaki and R. M. Laine, Organic/Inorganic Nanocomposite Star Polymers via Atom Transfer Radical Polymerization of Methyl Methacrylate Using Octafunctional Silsesquioxane Cores, *Macromolecules*, 2001, **34**, 5398–5407.
75 J. Pyun, K. Matyjaszewski, T. Kowalewski, D. Savin, G. Patterson, G. Kickelbick and N. Huesing, Synthesis of Well-Defined Block Copolymers Tethered to Polysilsesquioxane Nanoparticles and Their Nanoscale Morphology on Surfaces, *J. Am. Chem. Soc.*, 2001, **123**, 9445–9446.
76 F. J. Feher, D. Soulivong, A. G. Eklund and K. D. Wyndham, Cross-methathesis of alkenes with vinyl-substituted silsesquioxanes and spherosilicates: a new method for synthesizing highly-functionalized Si/O frameworks, *Chem. Commun.*, 1997, 1185–1187.
77 D. Neumann, M. Fisher, L. Tran and J. G. Matisons, Synthesis and Characterization of an Isocyanate Functionalized Polyhedral Oligosilsesquioxane and the Subsequent Formation of an Organic–Inorganic Hybrid Polyurethane, *J. Am. Chem. Soc.*, 2002, **124**, 13998–13999.
78 C. Zhang, F. Babonneau, C. Bonhomme, R. M. Laine, C. L. Soles, H. A. Hristov and A. F. Yee, Highly Porous Polyhedral Silsesquioxane Polymers. Synthesis and Characterization, *J. Am. Chem. Soc.*, 1998, **120**, 8380–8391.
79 R. M. Laine, J. Choi and I. Lee, Organic–Inorganic Nanocomposites with Completely Defined Interfacial Interactions, *Adv. Mater.*, 2001, **13**, 800–803.
80 J. Choi, J. Harcup, A. F. Yee, Q. Zhu and R. M. Laine, Organic/inorganic hybrid composites from cubic silsesquioxanes, *J. Am. Chem. Soc.*, 2001, **123**, 11420–11430.
81 J. Choi, A. F. Yee and R. M. Laine, Organic/Inorganic Hybrid Composites from Cubic Silsesquioxanes. Epoxy Resins of Octa(dimethylsiloxyethylcyclohexylepoxide) Silsesquioxane, *Chem. Mater.*, 2003, **15**, 5666–5682.
82 J. Choi, S. G. Kim and R. M. Laine, Organic/Inorganic Hybrid Epoxy Nanocomposites from Aminophenylsilsesquioxanes, *Macromolecules*, 2004, **37**, 99–109.
83 J. Choi, A. F. Yee and R. M. Laine, Toughening of cubic silsesquioxane epoxy nanocomposites using core shell rubber particles; a three component hybrid system, *Macromolecules*, 2004, **37**, 3267–3276.
84 D. Hoebbel, I. Pitsch and D. Heidemann, Inorganic organic polymers with defined silicic acid units,'' in *Eurogel '91*, ed. S. Vilminot, R. Nass and H. Schmidt, Elsevier Science Publishers, Amsterdam, 1992, pp. 467–473.
85 P. G. Harrison and R. Kannengiesser, Porous materials derived from trigonal-prismatic $[Si_6O_9]$ and cubane $[Si_8O_{12}]$ cage monomers, *Chem. Commun.*, 1996, 415.
86 M. Seino and Y. Kawakami, Selective Vinyl Functionalization of Octakis(dimethylsiloxy)octa-silsesquioxane with Allylbenzene and 1,5-Hexadiene and Copolymerization with Allybenzene and 1,5-Hexadiene and Copolymerization of the products with Bis(dimethylsilyl-benzene), *Polym. J.*, 2004, **36**, 422–429.
87 K. Su, D. R. Bujalski, K. Eguchi, G. V. Gordon, D.-L. Ou, P. Chevalier, S. Hu and R. P. Boisvert, Low-k Interlayer Dielectric Materials: Synthesis and Properties of Alkoxy-Functional Silsesquioxanes, *Chem. Mater.*, 2005, **17**, 2520–2529.
88 C. V. Nguyen, K. R. Carter, C. J. Hawker, J. L. Hedrick, R. L. Jaffe, R. D. Miller, J. F. Remenar, H.-W. Rhee, P. M. Rice, M. F. Toney, M. Trollsas and D. Y. Yoon, Low-Dielectric, Nanoporous Organosilicate Films Prepared via Inorganic/Organic Polymer Hybrid Templates, *Chem. Mater.*, 1999, **11**, 3080–3085.
89 N. Takamura, L. Viculis and R. M. Laine, A completely discontinuous organic/inorganic hybrid nanocomposite based on reactions of $[HMe_2SiOSiO_{1.5}]_8$ with vinylcyclohexene, to be submitted.

90 R. M. Laine, L. Viculis, N. Takamura and K. Shinotani, Self-curing silsesquioxane macromonomers for the solvent free processing of high temperature and air stable, transparent films, patent pending.
91 S. A. Pellice, D. P. Fasce and R. J. J. Williams, Properties of epoxy networks derived from the reaction of diglycidyl ether of bisphenol A with polyhedral oligomeric silsesquioxanes bearing OH-functionalized organic substituents, *J. Polym. Sci. B: Polym. Phys.*, 2003, **41**, 1451–61.
92 J. C. Huang, Y. Xiao, K. Y. Mya, X. M. Liu, C. B. He, J. Dai and Y. P. Siow, Thermomechanical properties of polyimide-epoxy nanocomposites from cubic silsesquioxane epoxides, *J. Mater. Chem.*, 2004, **14**, 2858–2863.
93 K. Y. Mya, C. B. He, J. C. Huang, Y. Xiao, J. Dai and Y. P. Siow, Preparation and thermomechanical properties of epoxy resins modified by octafunctional cubic silsesquioxane epoxides, *J. Polym. Sci. A: Polym. Chem.*, 2004, **42**, 3490–3503.